Feeding and Risering of High-Alloy Steel Castings

SHOUZHU OU, KENT D. CARLSON, and CHRISTOPH BECKERMANN

A more accurate, less conservative set of feeding distance (FD) and riser sizing rules is developed for high-alloy steel castings produced from alloy grades CF-8M, CA-15, HH, HK, and HP. These rules are designed to produce radiographically sound castings at 2 pct sensitivity. By comparing results between plate casting trials and the corresponding simulations of those trials, a relationship is shown to exist between a local thermal parameter known as the Niyama criterion and ASTM shrinkage X-ray level. This relationship is then used in an extensive set of casting simulations to numerically determine FDs for a wide range of casting conditions. It is shown that the FD rule developed in an analogous earlier study for carbon and low-alloy (C&LA) steels can also be used for these high-alloy grades, provided that the FD is modified by a multiplier that accounts for the high-alloy steel grade. In addition, it is shown that multipliers for superheat, sand mold material, and the use of chills developed in the earlier work are also valid with these high-alloy steel grades. In comparison with previously published high-alloy FD rules, the present rules are shown to provide longer FDs (and hence higher casting yields) in most casting situations. This study also investigates riser sizing rules. It is determined that for open top risers, the previously published C&LA riser sizing rule is also valid for high-alloy steels. This rule is less conservative than existing high-alloy riser sizing rules, specifying smaller risers that produce higher casting yields. In addition, for vented blind top risers, it is shown that the previously published rules are also overly conservative.

I. INTRODUCTION

MAXIMIZING casting yield, which is defined as the weight of a casting divided by the weight of the metal poured to produce the casting (*i.e.*, including metal that solidifies in the risers, gating, downsprue, *etc.*), is an important consideration in the steel casting industry. An increase in casting yield decreases production costs; with increased yield, production of the same number of castings requires less melted metal and fewer heats, as well as reduced labor and material costs required for production. Also, higher yield usually has the side benefit of lower casting cleaning costs. One effective way to improve casting yield is through riser optimization, where "optimized" means (1) the riser has the minimum possible volume to provide sufficient feed metal to the casting, without the riser pipe extending into the casting; and (2) the smallest number of risers are used, while still ensuring that the risers are close enough to each other to produce a sufficiently sound casting.

Computer simulation of the casting process is becoming an indispensable tool in the effort to increase casting yield. Through the use of simulation, foundries are able to evaluate modifications to casting designs without having to actually produce the casting, thus saving time, material resources, and manpower. However, computer simulation must be applied on a case-by-case basis, and its effective use requires expertise as well as accurate data for many process variables. Due to these limitations, risering rules are still widely used in the steel casting industry. Risering rules dictate riser size and placement by determining (1) the riser size necessary to supply adequate feed metal to a casting section, and (2) the feeding distance (FD), which is the maximum distance over which a riser can supply feed metal to produce a sound casting. A recent survey indicates that simulation is used for less than 10 pct of the tonnage of steel castings produced, and that risering rules (or rules-based software) are used to rig about 80 pct of the tonnage produced.[1,2] Due to the prevalence of rules-based rigging in the steel casting industry, any attempt to increase casting yield in a general sense must begin with these rules. Even if simulation is used, risering rules are still useful to develop a reasonable starting point for simulation, which will shorten the iterative optimization cycle.

A great deal of effort has been expended to develop rules for determining riser FDs in steel castings. Many researchers have developed empirical relations for determining feeding distances in carbon and low-alloy (C&LA) steels. These rules are typically based on experimental casting trials performed in the 1950s by Bishop, Myskowski, and Pellini at the Naval Research Laboratory (NRL),[3–7] as well as on similar casting trials conducted by the Steel Founders' Society of America (SFSA).[8] An extensive review of empirical FD relations for C&LA steels is provided in previous work by the current authors.[9,10] The numerical determination of FDs for C&LA steels has also been investigated. One of the earliest efforts was undertaken by Spiegelberg,[11,12] Maier,[13] and Ghun,[14] under the direction of Professor J.F. Wallace. This work theorized that shrinkage porosity would form in castings in locations where the solidification gradient near the end of solidification dropped below some minimum value. They determined the minimum value by comparing their numerical results to the NRL casting trial results.[3–7]

To the authors' knowledge, the only extensive research effort to develop FD rules specifically for high-alloy steels was performed by Varga *et al.*[15–18] Varga *et al.* began with the shape factor (SF) concept first proposed by Bishop and

SHOUZHU OU, Postdoctoral Research Associate, KENT D. CARLSON, Assistant Research Engineer, and CHRISTOPH BECKERMANN, Professor, are with the Department of Mechanical and Industrial Engineering, The University of Iowa, Iowa City, IA 52242. Contact e-mail: becker@engineering.uiowa.edu

co-workers[3–5,7] and Pellini[6] the SF of a casting section is calculated from the section's length, width, and thickness according to the relation SF = $(L + W)/T$. Varga *et al.* developed empirical charts that gave the appropriate riser size and FD for a given SF, assuming the riser was centrally located on the casting section. Their empirical data were obtained by performing a set of high-alloy casting trials. They cast plates in 16 foundries, in CF-8, CA-15, HH, HF, and HT alloy grades (including multiple compositions of several grades). All plates were cast with blind risers. Feeding distances were determined by finding the maximum length that a riser could feed to produce a sound casting, where soundness was defined as no visible shrinkage on radiographs filmed at 1.5 pct sensitivity. The end result of this work for top-risered castings is two empirical FD charts: one for blind risers feeding 1.27-cm (0.5-in.) thick sections and one for blind risers feeding 2.54-cm (1-in.) thick sections. An important note regarding these high-alloy FD charts is that the FD is defined from the center of the riser to the edge of the casting, rather than from the edge of the riser to the edge of the casting, as in the earlier C&LA rules (Figure 1). These inconsistent definitions make direct comparison of C&LA and high-alloy FDs from the literature difficult.

Considerable research has also been done to develop riser sizing guidelines for steel castings. Early quantitative approaches developed by Chvorinov[19] and Janco[20] allowed a foundry engineer to determine the riser size necessary to ensure that the riser would solidify after the casting section it was feeding. These methods were based on the work of Chvorinov,[21] who found that solidification time was directly related to a casting's volume-to-surface-area ratio. While these methods provided a riser that solidified after the casting, they did not ensure that the casting would be free from underriser shrinkage. Wlodawer[22] termed Chvorinov's volume-to-surface-area ratio the "solidification modulus," and developed the modulus method. According to his method, if the modulus of the riser is 20 pct larger than the modulus of the casting section to be fed, the riser will be sufficient and free from under-riser shrinkage. The modulus method is valid for both C&LA and high-alloy steels, primarily because it employs a significant factor of safety. Ruddle[23] modified Wlodawer's method by

explicitly accounting for the volumetric shrinkage of the casting section, which reduces the factor of safety somewhat to provide a more optimized riser size.

Caine[24] developed a riser sizing method for C&LA steels that also ensures castings free from under-riser shrinkage, by determining adequate riser size from an empirical relationship between the riser-volume-to-casting-volume ratio and a "freezing ratio," which is the surface-area-to-volume ratio of the casting divided by that of the riser. A disadvantage to this method is that it requires trial-and-error; one simply guesses a riser size, performs the calculations, and checks whether the size selected is adequate. If not, a larger size is chosen, and the calculations are repeated. This disadvantage was overcome in a method proposed by Bishop *et al.*,[25] who developed a direct method for determining riser size in C&LA steels. They replaced Caine's freezing ratio with a SF for the casting section to be fed (as discussed previously, SF = $(L + W)/T$). Once the SF for a casting section is calculated, the riser size can be directly determined through an empirical relation. They developed this empirical relation for riser height-to-diameter ratios from 0.5 to 1, and stated that a ratio larger than one decreases yield without providing additional benefits, while a ratio smaller than 0.5 produces a riser with a relatively large diameter that requires excessive cleaning costs to remove. They also provided a method to modify the riser size for complex-shaped castings (*i.e.*, casting sections with appendages).

As was the case for high-alloy feeding distance rules, the only extensive effort to develop riser sizing rules for high-alloy steels is the work of Varga *et al.*[15–18] In their casting trials, they used blind risers that had height-to-diameter ratios of one. They used the SF concept of Bishop *et al.*,[25] but Varga *et al.* determined the sufficient/minimum riser volume (and hence diameter and height, since $H/D = 1$) in a somewhat different manner than did Bishop *et al.* After determining the appropriate riser sizes for all the experimental castings, Varga *et al.* developed relations to directly determine riser size, based on the SF of the section to be fed. As with their FD rules, these riser sizing rules were developed for high-alloy grades CF-8, CA-15, HH, HF, and HT. Analogous to the work of Bishop *et al.*, they also provided a method to modify the riser size for complex-shaped high-alloy casting sections. For several reasons, the riser sizing methodology of Varga *et al.* is more conservative than that of Bishop *et al.*; this will be discussed in further detail in Section IV.

In 1973, the SFSA compiled the available low-alloy FD rules (the results from the NRL[3–7] and SFSA[8] casting trials and the numerical predictions performed at Case Western Reserve University[11–14]), the low-alloy riser sizing rules of Bishop *et al.*,[25] and the high-alloy FD and riser sizing rules developed by Varga *et al.*[15–18] into a handbook entitled *Risering Steel Castings*.[26] The data in this handbook, presented as charts, nomographs, equations, and procedures for risering steel castings, are intended to assist foundry engineers in the placement and sizing of risers on production steel castings. Although this handbook is 30 years old, it is still used in foundry practice today. However, there has been substantial feedback from SFSA member foundries indicating that the risering rules contained in *Risering Steel Castings*, while adequate, are often overly conservative.[1] Also, it was noted that these rules do not account for differences
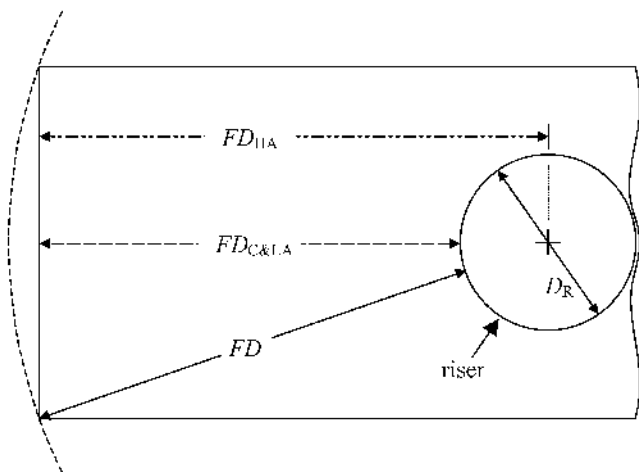

Fig. 1—Alternate definition of FD for previous high-alloy (FD_{HA}) rules, as well as the FD in the current work (FD), which extends from the edge of the riser to the furthest point in the casting.

in sand mold material, alloy composition (for low-alloy steels), or superheat, all of which are known to affect the distance over which a riser can provide feed metal to a casting section. For high-alloy steels, superheat is particularly important, as foundries typically use significantly larger superheats for high-alloy steels than for low-alloy steels.

To address the need for more accurate, less conservative risering rules, the present authors recently developed a new set of C&LA feeding distance rules.[9,10] The methodology underlying these rules is based on the Niyama criterion,[27] which is a local thermal parameter defined as $Ny = G/\sqrt{\dot{T}}$, where G is the temperature gradient and $\dot{T}$ is the cooling rate. By comparing radiographic testing (RT) casting soundness results from an extensive set of plate casting trials with Niyama criterion values computed from simulations corresponding to each casting trial, a correlation was found between casting soundness and the minimum Niyama criterion value. It was determined that, if the minimum Niyama value of a casting section is greater than 0.1 $K^{1/2} s^{1/2} mm^{-1}$, the section will be radiographically sound (i.e., no shrinkage visible on X-ray) at 2 pct sensitivity. This information was then used to develop rules for both end-effect FD and lateral FD for top risers, as well as FD for side risers. In addition, multipliers were developed to apply these rules with end chills and drag chills, as well as to tailor the rules to different C&LA steel alloy compositions, sand mold materials, and pouring superheats. These new rules provide longer FDs than previously published rules in most casting situations. The C&LA riser sizing methodology of Bishop et al.[25] was not revised, because it was found to be adequate (i.e., not overly conservative). These rules were also published in an SFSA report[28] that was distributed among SFSA member foundries. It should be noted that, although these FD rules (as well as all previous FD rules in the literature) were developed based on empirical data gathered from simple plate-shaped castings, the rules are also valid for more complex-shaped production castings. The rules are applied to production castings by dividing these more complex geometries into a series of at least approximately platelike shapes, and then applying the rules to these simpler shapes.

The objective of the present study is to develop a new, less conservative set of riser FD rules for common high-alloy steel grades. The approach taken is completely analogous to the present authors' C&LA FD rule development just discussed. High-alloy casting trials are coupled with simulation to establish the correlation necessary to develop high-alloy FD rules. In addition, high-alloy riser sizing rules are examined; based on this investigation, less conservative riser sizing rules are suggested. The use of these new high-alloy rules provides less conservative riser sizes and FDs in most instances, which will increase high-alloy casting yield. Note that the present study does not consider "necked-down" risers, where the riser casting surface contact area is reduced to enable easier riser removal after the casting has solidified, nor does it consider risers insulated with sleeves.

II. FD TERMINOLOGY

Before discussing the development of the FD rules, it is prudent to carefully define the terms that will be used for this development. The FD is defined as the maximum distance over which the riser can provide feed metal resulting in a radiographically sound casting. In the case of the SFSA guidelines for high-alloy steels, FD is defined from the center of the riser to the edge of the casting section (FD_{HA} in Figure 1), and soundness is defined as class I soundness at 1.5 pct radiographic sensitivity.[26] Class I soundness implies that some shrinkage is allowable, provided it is less severe than in the ASTM class I standard radiographs. For the present study, FD is defined from the edge of the riser to the furthest point in the casting section (FD in Figure 1), and soundness is defined as radiographically sound (i.e., no shrinkage visible on X-ray) at 2 pct sensitivity. Another way to explain how the FD is measured in the present study is to draw a circle centered about the riser with a radius equal to the FD plus the riser radius (Figure 1). Then, the casting section inside the circle is fed by that riser. It is noteworthy that this definition of FD is the same as the one used by the present authors in their earlier C&LA FD rule development;[9,10,28] the importance of this consistency will become evident when the high-alloy FD rules are developed.

A similar term that will be commonly used in this work is feeding length (FL). The FL of a casting section is simply the distance from the riser to the furthest point in the section. It is the length to be fed. It is purely geometrical, and implies nothing about the soundness of the casting section being fed. If the FL is less than or equal to the FD, the casting section will be sound; if the FL exceeds the FD, the casting section is likely to have visible shrinkage porosity.

There are two other terms that are important to understand when considering FDs: riser zone and end zone. Since the riser remains hotter than the casting section to be fed, it provides a temperature gradient that facilitates feeding. The length over which this riser effect acts to prevent shrinkage porosity is called the riser zone length (RZL), which is measured radially outward from a riser. This is illustrated for a top riser in Figure 2. The cooling effect of the mold at the end of a casting section also provides a temperature gradient along the length of the casting section to be fed.
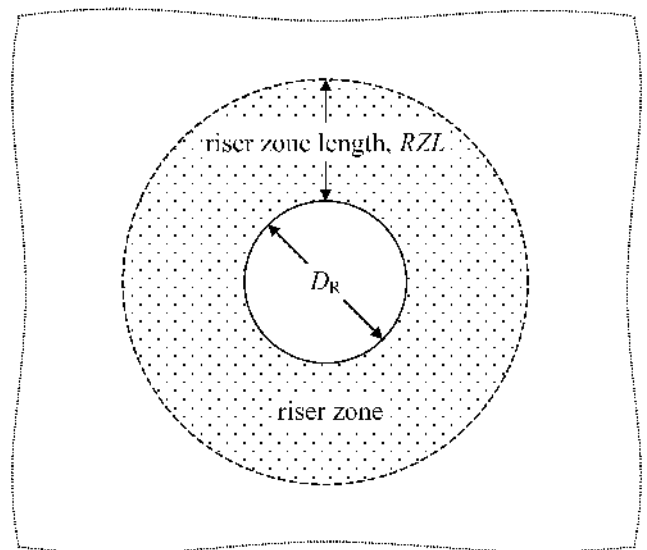

Fig. 2—Illustration of the RZL of a casting section without end effects; note that RZL is independent of the riser diameter D_R.
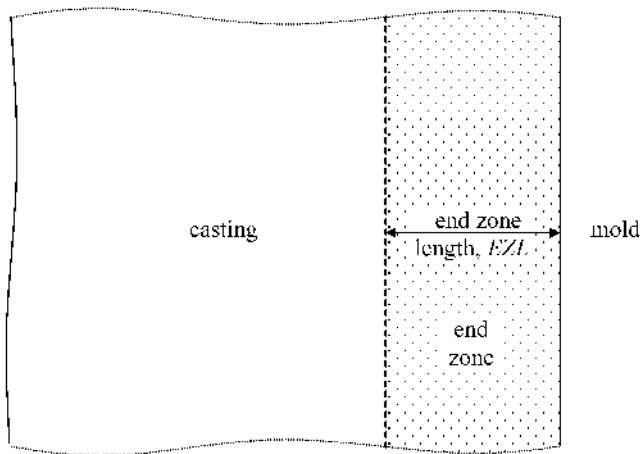
Fig. 3—Illustration of the EZL of a casting section.

This is called the end effect, and it produces a sound casting over the so-called end zone length (EZL), which is measured normal to the end of a casting section. This is depicted in Figure 3. The FD is a function of RZL and EZL. Put simply, for a casting section to be sound, the entire section must be within a riser zone or end zone region. If the FD is exceeded, shrinkage will begin to form in the region between the riser zone and the end zone. In reality, the relationship between FD, EZL, and RZL is more complicated; this is discussed in significant detail in the present authors' earlier C&LA work.[9,28]

III. HIGH-ALLOY PLATE CASTING TRIALS

As part of the present study, four different foundries cast a total of 165 high-alloy plates with a single top riser. The casting trial data are summarized in Table I. The alloys cast were CF-8M (125 plates), HH (20 plates), and HP (20 plates). The original intent was to also cast plates from CA-15 and HK, but the foundries that had agreed to perform those trials had to withdraw from the project. It will be shown in Section III, however, that it was possible to develop rules for these alloys without performing their casting trials. The general casting configurations used for high-alloy plate trials are shown in Figure 4; one set of plates (25 CF-8M plates) was cast vertically (Figure 4(b)), and the rest horizontally (Figure 4(a)). Again, recall that the FLs shown in Figure 4 are purely geometrical, and imply nothing about casting soundness. The casting trial plates are categorized into four groups, based on their width-to-thickness (W/T) ratio: W/T = 2, 5.5, 8, and 12. The W/T = 5.5 and 8 plates were 2.54-cm (1-in.) thick, while the W/T = 2 and 12 plates were 1.27-cm (0.5-in.) thick. The plate lengths (L), riser diameters (D_R), and riser heights (H_R) used for each plate are provided in Table I. Plate lengths were selected to produce plates ranging from radiographically sound to ASTM shrinkage X-ray level 5 (very unsound). The riser height-to-diameter ratios were all designed to be unity (H_R/D_R = 1); this was approximately achieved in practice, except for the W/T = 2 and W/T = 12 plates, where the casting foundry decided to use H_R/D_R ratios of 4.67 and 3, respectively. All of the plates described previously were cast in either PUNB (furan) or green sand molds.

When conducting the casting trials, it was envisioned that the trials would include the normal variations in casting conditions that are possible in foundry practice. These variations would then be considered in the analysis of the results. Therefore, detailed information was collected on the casting process for the trial plates, and all information was recorded in detailed data sheets that were filled out by the participating foundries. The casting parameters that were recorded were pouring temperature, pouring time, steel chemistry, mold material, actual casting rigging, and mold-box geometry. In addition, each plate cast in these trials was examined by RT according to ASTM E94[29] procedures, using E446[30] reference radiographs (for casting sections up to 5.08-cm (2-in.) thick). Based on this examination, an ASTM shrinkage RT level was assigned to each plate.

The results of the casting trials are given in Figures 5 through 8, which plot the FLs of the W/T = 2, 12, 5.5, and 8 plates, respectively, against the resulting ASTM shrinkage X-ray level for each corresponding plate. The different hollow symbols indicate plates cast by different foundries. When a number appears next to a symbol (or group of overlapping symbols), this indicates the number of plates of that FL with the same X-ray level. The shrinkage X-ray levels in these figures range from 0 to 5, where level 0 indicates that the plate was radiographically sound (*i.e.*, absolutely no indications visible on X-ray). While level 0 is not a standard ASTM X-ray level, it is used in this study because it provides additional information. Also shown in these figures are the mean X-ray level for each value of FL, as well as error bars indicating one standard deviation. The mean values and error bars are not intended to provide meaningful statistical data—the number of plates at each FL is generally small, and X-ray levels are quantized rather than continuous data—rather, they are provided to more clearly indicate the trends in the data.

Figures 5 and 6 show the results for the 1.27-cm (0.5-in.) thick plates. Some plate lengths were chosen for both of these sets of plates that are well in excess of the existing high-alloy FD rules for 1.27-cm (0.5-in.) plates, in an attempt to produce unsound plates with X-ray levels between 1 and 5. However, all the plates represented in Figures 5 and 6 have shrinkage levels of 0 or 1. The sound radiographic results of these casting trials are not entirely surprising; it is known that, for thin casting sections (*i.e.*, less than 2.54-cm (1-in.) thick), the FD becomes highly dependent on the filling process.[26] If a thin section is gated through the riser, FDs substantially longer than those predicted with rules for thicker sections can be achieved.[3] This phenomenon can be understood through casting simulation (using the methodology to determine FD, RZL, and EZL described in Section V). Gating through the riser enhances FD by increasing the RZL; it has little effect on the EZL. This increase in RZL is moderate for castings that have thickness 2.54 cm (1 in.) or larger, but becomes considerable when the thickness decreases to 1.27 cm (0.5 in.).

Figures 7 and 8 show the results for the 2.54-cm (1-in.) thick plates. Notice that, as plate length increases, the average shrinkage X-ray level tends to increase as well. An interesting feature of the casting trial results visible in these figures is the spread of X-ray levels for a given FL. Notice that there are several instances in Figures 7 and 8 where the range of X-ray levels at a given FL varies by three to five levels. This is particularly evident in Figure 8. This scatter is partially due to the variability in the casting process. Steel composition,

Table I. Experimental Data from the High-Alloy Plate Casting Trials

W/T*	Steel Alloy	Foundry	L (in.)	D_R (in.)	H_R (in.)	FL (in.)	Pouring T (°C)	Superheat (°C)	Sand Mold	X-Ray Level
2	CF-8M	A	3.25	1.5	7	1.80	1593.3	161.1	furan	0
2	CF-8M	A	3.25	1.5	7	1.80	1604.4	172.2	furan	0
2	CF-8M	A	3.25	1.5	7	1.80	1598.9	166.7	furan	0
2	CF-8M	A	3.25	1.5	7	1.80	1587.8	155.6	furan	0
2	CF-8M	A	3.25	1.5	7	1.80	1596.1	163.9	furan	0
2	CF-8M	A	3.75	1.5	7	2.29	1557.2	122.6	furan	0
2	CF-8M	A	3.75	1.5	7	2.29	1554.4	119.8	furan	0
2	CF-8M	A	3.75	1.5	7	2.29	1571.1	136.5	furan	0
2	CF-8M	A	3.75	1.5	7	2.29	1560.0	125.4	furan	0
2	CF-8M	A	3.75	1.5	7	2.29	1562.8	128.2	furan	0
2	CF-8M	A	4.75	1.5	7	3.28	1576.7	142.1	furan	0
2	CF-8M	A	4.75	1.5	7	3.28	1571.1	136.5	furan	0
2	CF-8M	A	4.75	1.5	7	3.28	1565.6	131.0	furan	0
2	CF-8M	A	4.75	1.5	7	3.28	1586.7	152.1	furan	0
2	CF-8M	A	4.75	1.5	7	3.28	1582.2	147.6	furan	0
2	CF-8M	A	6.75	1.5	7	5.27	1554.4	119.8	furan	1
2	CF-8M	A	6.75	1.5	7	5.27	1548.9	114.3	furan	1
2	CF-8M	A	6.75	1.5	7	5.27	1551.7	117.1	furan	0
2	CF-8M	A	6.75	1.5	7	5.27	1565.6	131.0	furan	1
2	CF-8M	A	6.75	1.5	7	5.27	1555.6	121.0	furan	1
5.5	CF-8M	F	7	4	3.5	7.0	1587.2	133.2	furan	0
5.5	CF-8M	F	7	4	3.5	7.0	1587.2	133.2	furan	0
5.5	CF-8M	F	7	4	3.5	7.0	1587.2	133.2	furan	0
5.5	CF-8M	F	7	4	3.5	7.0	1587.2	133.2	furan	0
5.5	CF-8M	F	7	4	3.5	7.0	1587.2	133.2	furan	0
5.5	CF-8M	F	9.4	4	3.5	9.4	1587.2	133.2	furan	2
5.5	CF-8M	F	9.4	4	3.5	9.4	1587.2	133.2	furan	2
5.5	CF-8M	F	9.4	4	3.5	9.4	1587.2	133.2	furan	0
5.5	CF-8M	F	9.4	4	3.5	9.4	1587.2	133.2	furan	3
5.5	CF-8M	F	9.4	4	3.5	9.4	1587.2	133.2	furan	3
5.5	CF-8M	F	12.3	4	3.5	12.3	1582.8	128.8	furan	3
5.5	CF-8M	F	12.3	4	3.5	12.3	1582.8	128.8	furan	3
5.5	CF-8M	F	12.3	4	3.5	12.3	1582.8	128.8	furan	4
5.5	CF-8M	F	12.3	4	3.5	12.3	1582.8	128.8	furan	2
5.5	CF-8M	F	12.3	4	3.5	12.3	1582.8	128.8	furan	4
5.5	CF-8M	F	15	4	3.5	15.0	1582.8	128.8	furan	5
5.5	CF-8M	F	15	4	3.5	15.0	1582.8	128.8	furan	5
5.5	CF-8M	F	15	4	3.5	15.0	1582.8	128.8	furan	5
5.5	CF-8M	F	15	4	3.5	15.0	1582.8	128.8	furan	5
5.5	CF-8M	F	15	4	3.5	15.0	1582.8	128.8	furan	5
5.5	CF-8M	F	18	4	3.5	18.0	1582.2	128.2	furan	5
5.5	CF-8M	F	18	4	3.5	18.0	1582.2	128.2	furan	5
5.5	CF-8M	F	18	4	3.5	18.0	1582.2	128.2	furan	5
5.5	CF-8M	F	18	4	3.5	18.0	1582.2	128.2	furan	5
5.5	CF-8M	F	18	4	3.5	18.0	1582.2	128.2	furan	5
5.5	CF-8M	K	11	4	4.5	7.41	1586.1	154.1	furan	0
5.5	CF-8M	K	11	4	4.5	7.41	1579.4	147.4	furan	0
5.5	CF-8M	K	11	4	4.5	7.41	1579.4	147.4	furan	0
5.5	CF-8M	K	11	4	4.5	7.41	1580.6	148.6	furan	0
5.5	CF-8M	K	11	4	4.5	7.41	1579.4	147.4	furan	0
5.5	CF-8M	K	12.5	4	4.5	8.85	1587.8	155.8	furan	0
5.5	CF-8M	K	12.5	4	4.5	8.85	1587.2	155.2	furan	0
5.5	CF-8M	K	12.5	4	4.5	8.85	1585.0	153.0	furan	0
5.5	CF-8M	K	12.5	4	4.5	8.85	1579.4	147.4	furan	0
5.5	CF-8M	K	12.5	4	4.5	8.85	1579.4	147.4	furan	0
5.5	CF-8M	K	14	4	4.5	10.3	1598.9	166.9	furan	2
5.5	CF-8M	K	14	4	4.5	10.3	1587.8	155.8	furan	3
5.5	CF-8M	K	14	4	4.5	10.3	1579.4	147.4	furan	0
5.5	CF-8M	K	14	4	4.5	10.3	1580.0	148.0	furan	0
5.5	CF-8M	K	14	4	4.5	10.3	1579.4	147.4	furan	0
5.5	CF-8M	K	16	4	4	12.3	1597.8	165.8	furan	1
5.5	CF-8M	K	16	4	4	12.3	1590.0	158.0	furan	3
5.5	CF-8M	K	16	4	4	12.3	1590.0	158.0	furan	2

W/T*	Steel Alloy	Foundry	L (in.)	D_R (in.)	H_R (in.)	FL (in.)	Pouring T (°C)	Superheat (°C)	Sand Mold	X-Ray Level
5.5	CF-8M	K	16	4	4	12.3	1587.8	155.8	furan	2
5.5	CF-8M	K	16	4	4	12.3	1582.2	150.2	furan	4
5.5	CF-8M	K	18.5	4	4	14.7	1596.1	164.1	furan	3
5.5	CF-8M	K	18.5	4	4	14.7	1593.9	161.9	furan	3
5.5	CF-8M	K	18.5	4	4	14.7	1590.6	158.6	furan	3
5.5	CF-8M	K	18.5	4	4	14.7	1590.0	158.0	furan	3
5.5	CF-8M	K	18.5	4	4	14.7	1581.7	149.7	furan	2
8	CF-8M	A	9	4	6	6.06	1595.6	167.1	furan	0
8	CF-8M	A	9	4	6	6.06	1580.6	152.1	furan	0
8	CF-8M	A	9	4	6	6.06	1590.6	162.1	furan	0
8	CF-8M	A	9	4	6	6.06	1587.8	159.3	furan	0
8	CF-8M	A	9	4	6	6.06	1593.3	164.8	furan	0
8	CF-8M	A	10	4	6	6.94	1558.9	123.4	furan	0
8	CF-8M	A	10	4	6	6.94	1570.6	135.1	furan	0
8	CF-8M	A	10	4	6	6.94	1548.9	113.4	furan	0
8	CF-8M	A	10	4	6	6.94	1560.0	124.5	furan	0
8	CF-8M	A	10	4	6	6.94	1554.4	118.9	furan	0
8	CF-8M	A	11	4	6	7.85	1557.2	125.0	furan	0
8	CF-8M	A	11	4	6	7.85	1551.7	119.5	furan	0
8	CF-8M	A	11	4	6	7.85	1576.7	144.5	furan	0
8	CF-8M	A	11	4	6	7.85	1565.6	133.4	furan	0
8	CF-8M	A	11	4	6	7.85	1582.2	150.0	furan	0
8	CF-8M	A	15	4	6	11.6	1605.6	170.1	furan	0
8	CF-8M	A	15	4	6	11.6	1604.4	168.9	furan	0
8	CF-8M	A	15	4	6	11.6	1593.3	157.8	furan	0
8	CF-8M	A	15	4	6	11.6	1582.2	146.7	furan	0
8	CF-8M	A	15	4	6	11.6	1576.7	141.2	furan	0
8	CF-8M	S	13	4	5.7	9.70	1552.2	120.2	green	4
8	CF-8M	S	13	4	3.8	9.70	1543.3	111.3	green	5
8	CF-8M	S	13	4	5.56	9.70	1553.9	121.9	green	5
8	CF-8M	S	13	4	5.22	9.70	1553.9	121.9	green	5
8	CF-8M	S	15	4	4.6	11.6	1552.2	120.2	green	3
8	CF-8M	S	15	4	4.8	11.6	1541.7	109.7	green	5
8	CF-8M	S	17	4	4.4	13.5	1551.7	119.7	green	5
8	CF-8M	S	17	4	4.8	13.5	1543.3	111.3	green	5
8	CF-8M	S	20	4	4.8	16.4	1551.7	119.7	green	5
8	CF-8M	S	20	4	5.9	16.4	1543.3	111.3	green	5
8	HH	A	11	4	4.25	7.85	1590.6	196.6	furan	0
8	HH	A	11	4	4.25	7.85	1590.6	196.6	furan	0
8	HH	A	11	4	4.75	7.85	1579.4	185.4	furan	0
8	HH	A	11	4	4.75	7.85	1579.4	185.4	furan	0
8	HH	A	13	4	4.125	9.70	1567.2	173.2	furan	1
8	HH	A	13	4	4.125	9.70	1567.2	173.2	furan	0
8	HH	A	13	4	4.25	9.70	1575.6	181.6	furan	0
8	HH	A	13	4	4.25	9.70	1575.6	181.6	furan	1
8	HH	A	15	4	4.5	11.6	1570.6	176.6	furan	2
8	HH	A	15	4	4.5	11.6	1570.6	176.6	furan	1
8	HH	A	15	4	4.5	11.6	1556.1	162.1	furan	1
8	HH	A	15	4	4.5	11.6	1556.1	162.1	furan	2
8	HH	A	17	4	4	13.5	1552.8	158.8	furan	1
8	HH	A	17	4	4	13.5	1552.8	158.8	furan	1
8	HH	A	17	4	4	13.5	1534.4	140.4	furan	1
8	HH	A	17	4	4	13.5	1534.4	140.4	furan	1
8	HH	A	20	4	4.25	16.4	1583.9	189.9	furan	1
8	HH	A	20	4	4.25	16.4	1583.9	189.9	furan	2
8	HH	A	20	4	3.75	16.4	1614.4	220.4	furan	4
8	HH	A	20	4	3.75	16.4	1614.4	220.4	furan	2
8	HP	A	11	4	4	7.85	1576.7	231.7	furan	0
8	HP	A	11	4	4	7.85	1576.7	231.7	furan	0
8	HP	A	11	4	4.5	7.85	1586.1	241.1	furan	0
8	HP	A	11	4	4.5	7.85	1586.1	241.1	furan	0
8	HP	A	13	4	4	9.70	1565.6	220.6	furan	2
8	HP	A	13	4	4	9.70	1565.6	220.6	furan	3

W/T*	Steel Alloy	Foundry	L (in.)	D_R (in.)	H_R (in.)	FL (in.)	Pouring T (°C)	Superheat (°C)	Sand Mold	X-Ray Level
8	HP	A	13	4	4.125	9.70	1565.6	220.6	furan	1
8	HP	A	13	4	4.125	9.70	1565.6	220.6	furan	1
8	HP	A	15	4	5	11.6	1597.2	252.2	furan	1
8	HP	A	15	4	5	11.6	1597.2	252.2	furan	2
8	HP	A	15	4	4.5	11.6	1602.8	257.8	furan	2
8	HP	A	15	4	4.5	11.6	1602.8	257.8	furan	2
8	HP	A	17	4	4	13.5	1536.7	191.7	furan	4
8	HP	A	17	4	4	13.5	1536.7	191.7	furan	5
8	HP	A	17	4	4.25	13.5	1585.6	240.6	furan	5
8	HP	A	17	4	4.25	13.5	1585.6	240.6	furan	5
8	HP	A	20	4	4.25	16.4	1598.9	253.9	furan	5
8	HP	A	20	4	4.25	16.4	1598.9	253.9	furan	5
8	HP	A	20	4	4.25	16.4	1607.8	262.8	furan	5
8	HP	A	20	4	4.25	16.4	1607.8	262.8	furan	5
12	CF-8M	A	4.4	2	6	3.53	1605.6	181.2	furan	0
12	CF-8M	A	4.4	2	6	3.53	1582.8	158.4	furan	0
12	CF-8M	A	4.4	2	6	3.53	1586.7	162.3	furan	0
12	CF-8M	A	4.4	2	6	3.53	1587.8	163.4	furan	0
12	CF-8M	A	4.4	2	6	3.53	1595.6	171.2	furan	0
12	CF-8M	A	5	2	6	4.00	1588.3	163.9	furan	0
12	CF-8M	A	5	2	6	4.00	1610.6	186.2	furan	0
12	CF-8M	A	5	2	6	4.00	1604.4	180.0	furan	0
12	CF-8M	A	5	2	6	4.00	1598.9	174.5	furan	0
12	CF-8M	A	5	2	6	4.00	1593.3	168.9	furan	0
12	CF-8M	A	5.7	2	6	4.58	1585.0	150.3	furan	0
12	CF-8M	A	5.7	2	6	4.58	1582.2	147.5	furan	0
12	CF-8M	A	5.7	2	6	4.58	1578.9	144.2	furan	0
12	CF-8M	A	5.7	2	6	4.58	1585.0	150.3	furan	0
12	CF-8M	A	5.7	2	6	4.58	1587.8	153.1	furan	0
12	CF-8M	A	7.2	2	6	5.89	1593.3	168.9	furan	1
12	CF-8M	A	7.2	2	6	5.89	1598.9	174.5	furan	1
12	CF-8M	A	7.2	2	6	5.89	1587.8	163.4	furan	1
12	CF-8M	A	7.2	2	6	5.89	1582.8	158.4	furan	1
12	CF-8M	A	7.2	2	6	5.89	1600.0	175.6	furan	1
12	CF-8M	A	9.2	2	6	7.73	1567.8	99.8	furan	1
12	CF-8M	A	9.2	2	6	7.73	1571.1	103.1	furan	0
12	CF-8M	A	9.2	2	6	7.73	1565.6	97.6	furan	1
12	CF-8M	A	9.2	2	6	7.73	1577.8	109.8	furan	0
12	CF-8M	A	9.2	2	6	7.73	1568.3	100.3	furan	0

*The W/T = 2 and 12 plates are 1.27-cm (0.5-in.) thick, and the W/T = 5.5 and 8 plates are 2.54-cm (1-in.) thick.
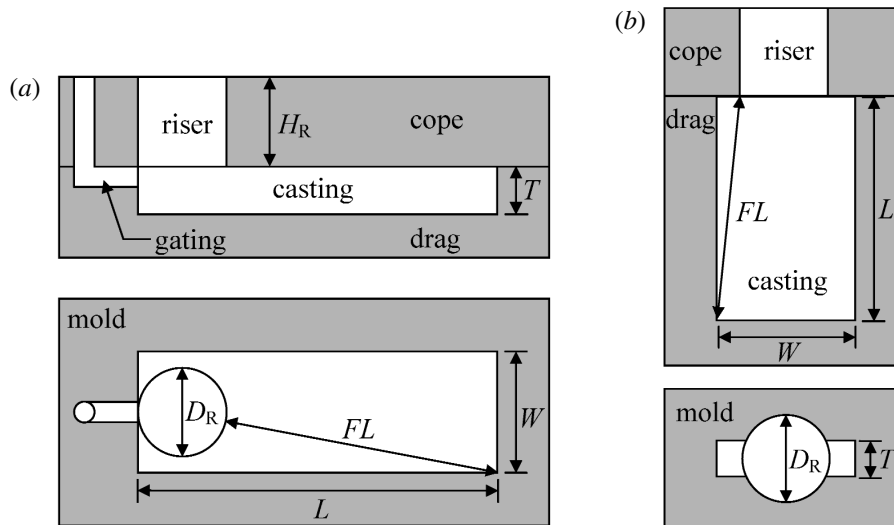
Fig. 4—General configuration and nomenclature for (a) horizontal and (b) vertical plate casting trials.
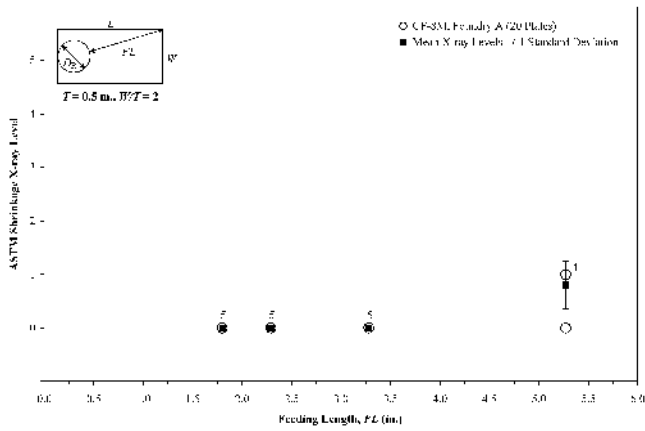
Fig. 5—Casting trial results for the $W/T = 2$ [1.27 by 2.54 cm (0.5-in. T by 1-in. W)] plates: soundness *vs* feeding length.
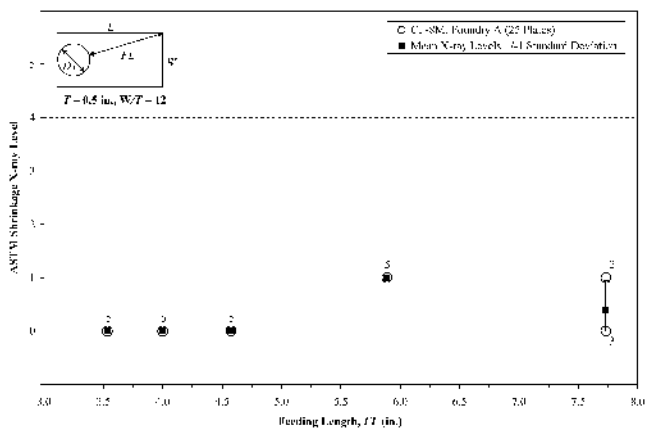
Fig. 6—Casting trial results for the $W/T = 12$ [1.27 by 15.2 cm (0.5-in. T by 6-in. W)] plates: soundness *vs* feeding length.
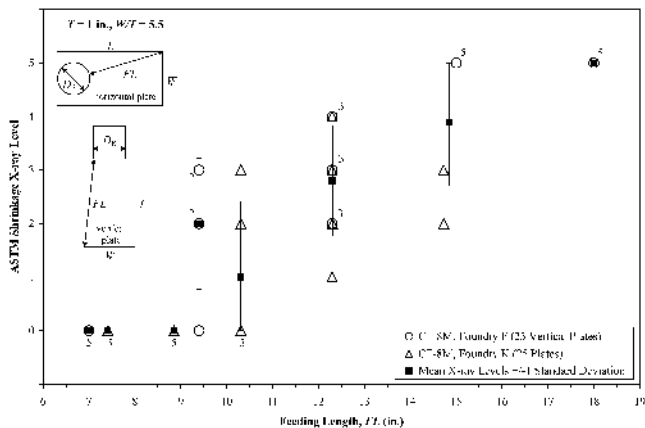

Fig. 7—Casting trial results for the $W/T = 5.5$ [2.54 by 14.0 cm (1-in. T by 5.5-in. W)] plates: soundness *vs* feeding length.

pouring temperature, pouring time, mold material, *etc.* varied from foundry to foundry. The effect of such differences in the production setting is visible in the results shown in Figures 7 and 8; notice that the variation in X-ray level at a given FL for a given alloy cast by one foundry is generally smaller
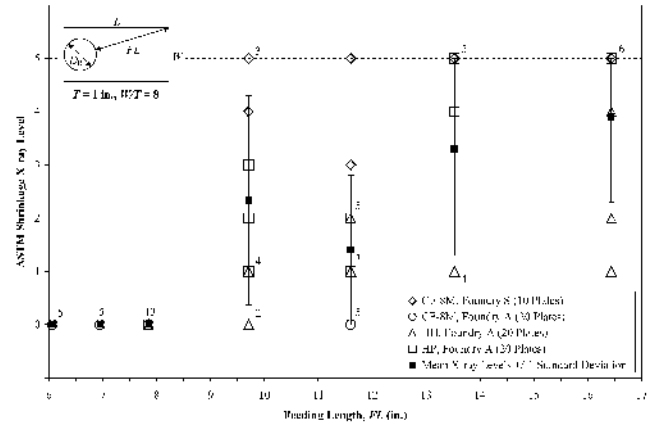
Fig. 8—Casting trial results for the $W/T = 8$ [2.54 by 20.3 cm (1-in. T by 8-in. W)] plates: soundness *vs* feeding length.

than the total variation at that FL. Some casting parameters (*e.g.*, pouring temperature) even varied to some degree within a single foundry. Another factor contributing to the scatter in X-ray level at a given FL is the variability inherent in assigning X-ray levels to a given radiograph (about $\pm$ 1.4 X-ray levels, on average[31]). A final cause of the scatter is the presence of gas porosity (of a spherical nature, and thus not considered in the shrinkage rating) in some of these plates.

IV. SIMULATION OF CASTING TRIALS

Based on the information given on the casting trial data sheets for the plates, simulations were performed for each plate for which unique casting data were available, using the commercial simulation software package MAGMASOFT.* By

---

*Although MAGMASOFT[32] was used in this work to simulate the casting trials, a number of simulation packages are available, and most of them are capable of calculating the Niyama criterion. In fact, the authors performed a comparison between MAGMASOFT and AFSolid,[33] and determined that the Niyama values calculated by these two packages for the same casting conditions are similar, provided that one takes care to ensure the Niyama values are calculated in the same manner (*e.g.*, evaluated at the same temperature), and that the values are converted to the same units.[34]

---

using this detailed casting information as input for the simulations, it was possible to account for the variability due to differences in casting parameters from foundry to foundry (and from plate to plate). Simulation of the filling process was included, to model the flow of the melt through the gating and into the castings, as well as the cooling of the metal that occurs during this process. The thermophysical properties of each steel alloy considered were computed using the interdendritic solidification computer software (IDS) developed by Miettinen *et al.*[35,36] The composition entered into IDS for each alloy was the average composition for that alloy reported by all foundries that cast the alloy during the trials. When using IDS, a cooling rate of 0.5 °C/s was assumed for all alloys. For the higher carbon content alloys (HH, HK, and HP, which have 0.30, 0.44, and 0.37 pct carbon, respectively), where carbide formation occurs toward the end of solidification, the solid fraction curves obtained by IDS were modified near the end of solidification. The reason for this is because IDS does not account for carbide formation, which raises the

solidus temperature. The solid fraction curves for these three alloys were modified by changing the solidus temperature to the carbide formation temperature, as given in the literature.[37] The solid fraction *vs* temperature and mixture density *vs* temperature curves for the alloys of interest are shown in Figure 9. Also included in this figure are the corresponding curves for a plain carbon steel (AISI 1025), for comparison. Three different CF-8M compositions were computed (with 0.03, 0.06, and 0.08 pct carbon), to correspond with the different compositions cast by the foundries involved. In Figure 9(a), note the similarity in the freezing ranges for these alloys; the curves shift to the left (to lower temperature ranges) as the amount of alloying elements increases, but the sizes are generally similar. However, Figure 9(b) shows that there are greater differences among these alloys in their density change during solidification (*i.e.*, solidification shrinkage). These differences in shrinkage contraction will be discussed in the riser sizing section.

Figure 9 can be used to explain the rationale behind developing feeding distance rules for HK and CA-15 alloys without performing those casting trials. The composition of HK is very similar to that of HH and HP, differing primarily in the nickel content. Fortunately, the nickel content of HK is between that of HH and HP. Thus, one would expect the thermophysical properties of HK to be similar to those of HH and HP. This is evident in Figure 9(a), where the solidification path of HK44 is seen to fall between HH and HP. Figure 9(b) shows that the density curves for these three alloys are very similar as well. Similarly, the composition of CA-15 falls between plain carbon steel and CF-8M. Figure 9 shows that both the solidification path and density curves of CA-15 fall between plain carbon steel and CF-8M values. Because the properties of HK and CA-15 lie between those of alloys that were cast in the casting trials (plain carbon steel plates were cast in the low-alloy casting trials[9]), and because the primary purpose of the casting trials was to validate the simulation results used to develop the FD rules, it was deemed acceptable to develop FD rules for HK and CA-15 based on simulation alone.
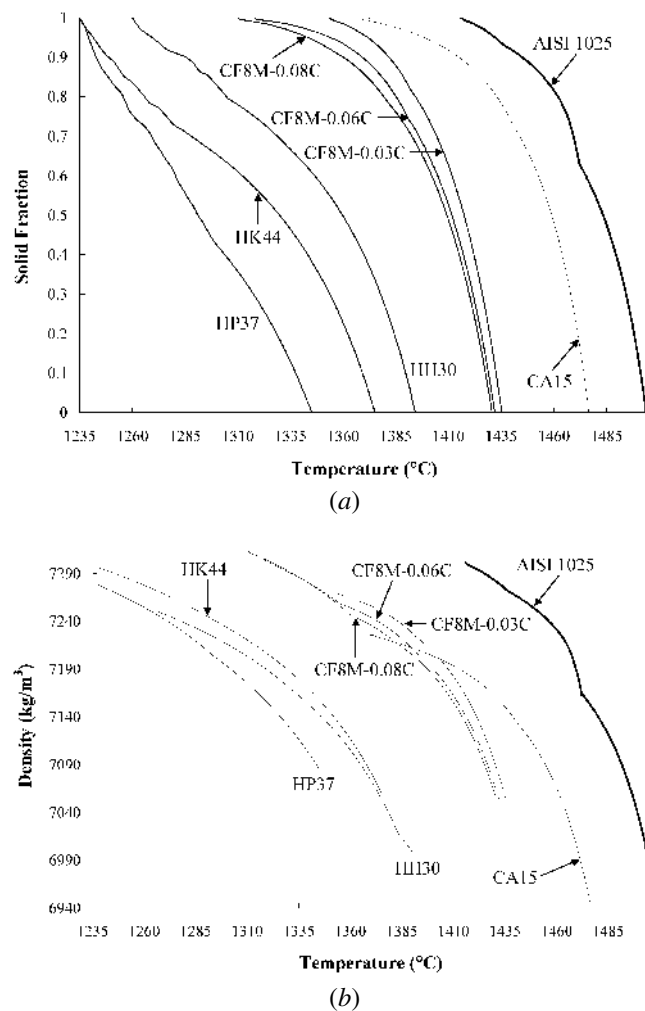
The simulations of the plate casting trials provided the distribution of the Niyama criterion throughout the castings. The Niyama criterion—defined as Ny = $G/\sqrt{\dot{T}}$, where G is the temperature gradient (in K/mm in the present work) and $\dot{T}$ is the cooling rate (in K/s)—is evaluated at the end of solidification, but different researchers use different interpretations of "end of solidification." In the present work, the temperature at which the Niyama criterion was evaluated was defined as 10 pct of the freezing range above the solidus temperature; this is the default definition used in MAGMASOFT. An example of the Niyama-value distribution in a typical plate is shown in Figure 10. This is a simulation of a 2.54 by 20.3 by 43.2 cm (1 by 8 by 17 in.) HH plate, which is long enough to exceed the FD for the riser (refer to the results for FL = 34.4 cm (13.5 in.) in Figure 9). In the casting trials, centerline shrinkage was commonly found in plates with these dimensions. Notice
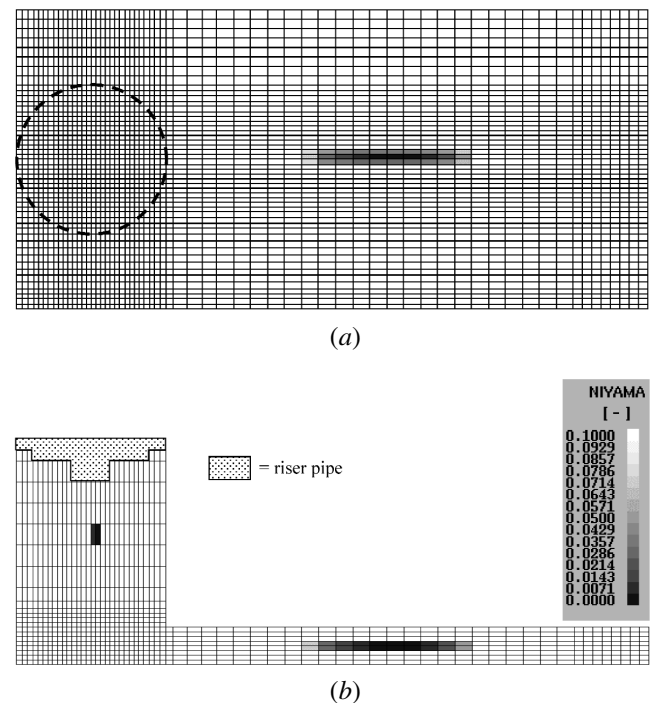

(a)

Fig. 9—Computed values for alloys of interest: (*a*) solid fraction and (*b*) density during solidification.

(b)

Fig. 10—Niyama value distribution in a 2.54 by 20.3 by 43.2 cm (1 by 8 by 17 in.) HH plate: (*a*) top view of central-thickness cross section and (*b*) side view of central-width cross section.

that, in both the top view (Figure 10(a)) and side view (Figure 10(b)) cross sections, the lowest Niyama values (*i.e.*, the darkest cells) are confined to the center of the plate. The region with the lowest Niyama values corresponds very closely to the region where centerline shrinkage occurs.

For each simulated plate, the minimum value of the Niyama criterion in the central-thickness cross section (*i.e.*, the plane one would see in a typical X-ray of the plate, Figure 7(a)) was determined. In addition, the total area in that same cross section with Niyama criterion values below some critical value was also recorded for each simulation. It is important to note that care must be taken when extracting Niyama values from simulation results. For example, in the present study, it was necessary to turn off the postprocessor's interpolation function (which is set "on" by default in MAGMASOFT) in order to determine the correct Niyama values for each metal cell of interest. Figure 11 plots the minimum Niyama values of the $W/T = 8$ plates against the FL of each plate. There is a very obvious trend of decreasing minimum Niyama values as the FL increases (and hence plate soundness decreases). Analogous plots for the $W/T = 2$, 5.5, and 12 plates look very similar to Figure 11; for this reason, they are not presented here.

Computational results such as those in Figure 11 can be combined with the experimental results shown in Figures 5 through 8 by eliminating the FL from these figures and simply plotting the ASTM shrinkage X-ray level determined for each plate *vs* the minimum Niyama value resulting from the simulation of that plate. In other words, one can plot the measured soundness, in terms of shrinkage X-ray level, against the predicted soundness, in terms of minimum Niyama value. This is shown in Figure 12, which includes all 165 high-alloy plates ($W/T = 2$, 5.5, 8 and 12) described in Section III. The first noteworthy feature of this figure is a definite tendency toward lower and lower minimum Niyama values as the X-ray level increases. This trend is highlighted in the plot inset in the upper-right corner of Figure 12, which shows the mean value of Ny_{min} for plates having X-ray levels from level 1 to level 4. The mean values for each X-ray level are shown with bars indicating the size of the range from minus one to plus one standard deviation from the mean. This is an indication of the scatter of the values for plates with a given X-ray level. No mean minimum Niyama values are given for level 0 or level 5 because the mean value for level 5 plates could be made almost arbitrarily small by casting a large number of very long plates, and the mean value for level 0 plates could similarly be made almost arbitrarily large by casting a large number of short plates. Note that the minimum Niyama value asymptotes to zero as the X-ray level increases to level 5, and that the scatter in Ny_{min} tends to decrease as the X-ray level increases.
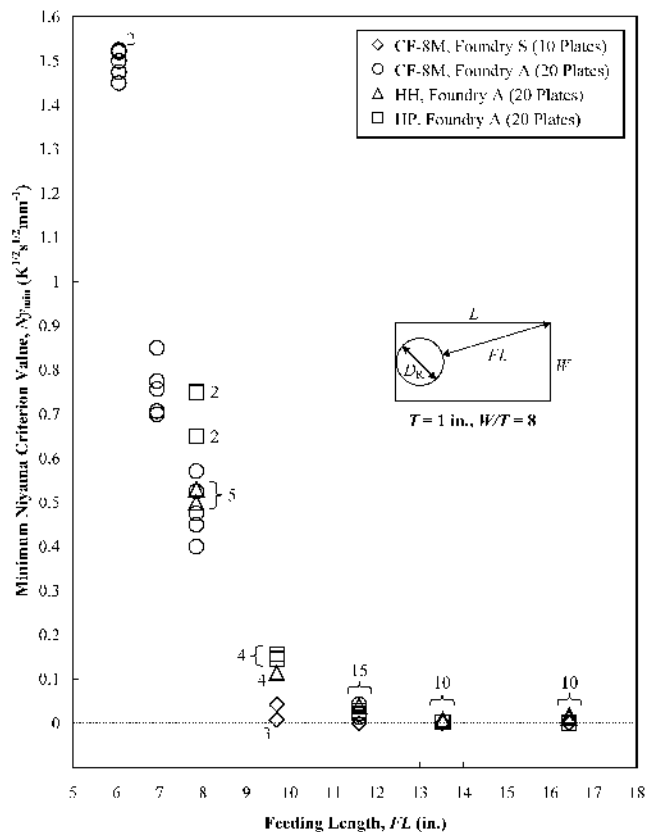
It is also apparent from Figure 12 that a plate with a relatively large value of Ny_{min} will have a low X-ray level. Note that all of the plates with a minimum Niyama value greater than 0.2 are level 1 or better, and almost all of the plates with $Ny_{min} > 0.1$ are level 1 or better. The two plates with $Ny_{min} > 0.1$ that have X-ray levels higher than level 1 are considered outliers; they are the result of (1) the previously mentioned scatter in the experimental data that could not be accounted for in the simulations and (2) differences between the actual casting conditions and the values that were recorded. As an example of the latter, if the recorded superheat were higher than the actual superheat, the simulation would result in a plate more sound (hence, with a larger Ny_{min}) than was produced in the trials. It is evident that there is a transition, as the Niyama value decreases to somewhere around 0.1 to 0.2, from radiographically sound plates to unsound plates. For the present study, it was desirable to define some threshold value to denote this transition. The value chosen as the threshold is $Ny_{min} = 0.1 \ K^{1/2} \ s^{1/2} \ mm^{-1}$. This is the same threshold value that was chosen for the C&LA FD rules developed by the present authors;[9] a thorough justification of the choice is provided in this earlier work.
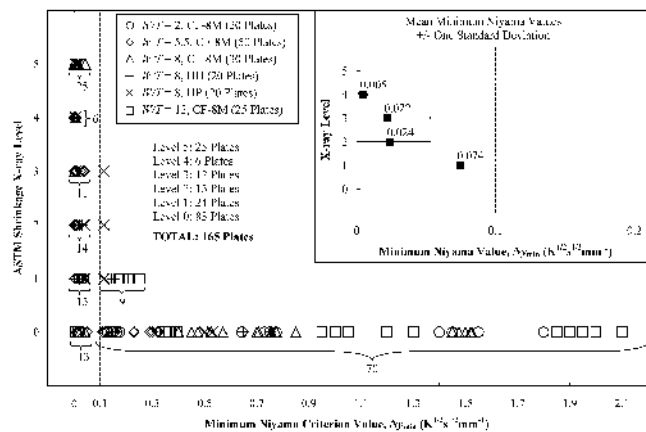

Fig. 11—Simulation results for the $W/T = 8$ plates: minimum Niyama value *vs* feeding length.

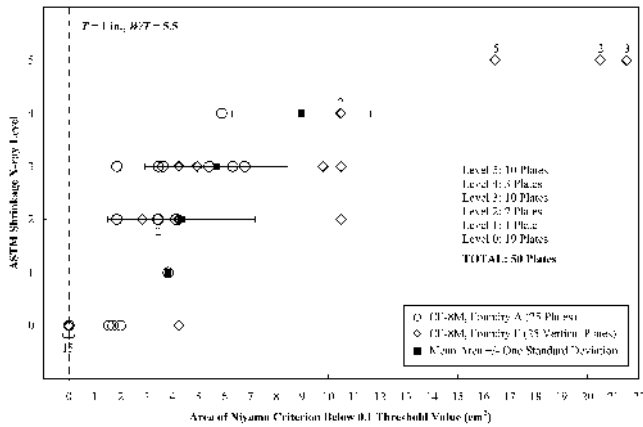Fig. 12—ASTM shrinkage X-ray level *vs* minimum Niyama criterion value for the $W/T = 2$, 5.5, 8, and 12 plates.

Fig. 13—Casting soundness *vs* area of cells below Niyama criterion threshold value of 0.1 (K s)$^{1/2}$/mm, for the $W/T = 5.5$ plates.

Fig. 14—Cross-section (*a*) side view and (*b*) top view Niyama plots from a simulation of a 7.62 by 15.2 by 52.6 cm (3-in. *T* by 6-in. *W* by 20.7-in. *L*) top-risered AISI 1025 steel plate.

While it is true that a relatively large Niyama value indicates that a plate will probably have a low X-ray level, the converse is not true: a small value of Ny_{min} does not necessarily imply that the corresponding plate will have a high X-ray level. This is evident from the large number of plates in the lower-left corner of Figure 12 that are level 1 or better, and yet have $Ny_{min} < 0.05$. Although this may appear troubling at first glance, it can be explained by considering Figure 12 in conjunction with Figure 13, which plots the shrinkage X-ray level of the $W/T = 5.5$ plates against the area of these plates with Niyama criterion values below the threshold value of 0.1, measured from the corresponding plate simulations (Figure 10(a)). Figure 13 includes the values for each individual plate (numbers next to symbols indicate multiple plates with the same value), as well as the mean area for all of the plates at each X-ray level plus/minus one standard deviation. As in Figure 12, no mean values are given for level 0 or level 5 in these figures, because the mean areas for these levels are rather arbitrary. An area of zero indicates that the minimum Niyama value is greater than 0.1. Figure 13 shows that, as the X-ray level of a plate increases, the area with Niyama values less than 0.1 tends to increase as well. The standard deviation bars show that there is a significant amount of scatter in these data. From Figure 13, it can be seen that the level 0 and level 1 plates in Figure 12 with $Ny_{min} < 0.1$ generally have very small areas with Niyama values less than 0.1. Thus, a small minimum Niyama value does not necessarily imply that the plate should have a high X-ray level; if the area with Ny < 0.1 is small, the plate may still be radiographically sound. The analogous plot for the $W/T = 8$ plates shows the same trends, and thus is not shown; the $W/T = 2$ and 12 plates all have X-ray levels of 0 or 1, so a plot of this type is not useful.

V. CALCULATION OF FD

At this point, it is necessary to revisit the C&LA FD rule development previously performed by the present authors.[9,10,28] The reason for this is that the high-alloy rules will be shown to be directly linked to the previously developed rules for C&LA steels. As mentioned earlier, the high-alloy rule development d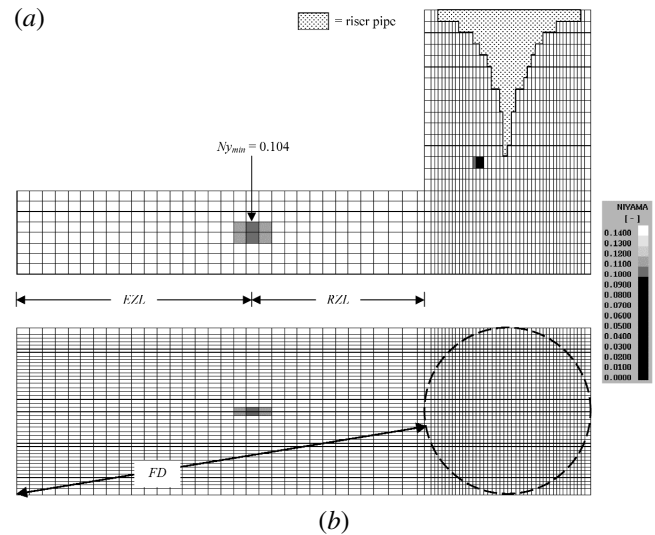escribed in this article was performed in a manner completely analogous to the development of the C&LA rules. Comparison between the C&LA casting trials and the simulations of those trials led to the same conclusion determined for high-alloy steels in Section V: if the minimum Niyama value in a casting section is greater than 0.1 K$^{1/2}$ s$^{1/2}$ mm^{-1}, the casting section should be radiographically sound. Once this relationship was established, a great number of casting simulations were performed. These simulations were run without considering filling; *i.e.*, the simulation began with the mold cavity full of metal at T_{pour}. Simulating without filling results in slightly shorter FDs, which means that the rules developed here are slightly conservative; however, the overall effect is very small. Simulations were performed using values of plate thickness *T* ranging from 2.54 to 30.5 cm (1 to 12 in.). For each thickness, plates were simulated with widths corresponding to *W/T* ratios ranging from 1 to 17. For each value of *T* and *W/T*, the plate length *L* was varied until the minimum Niyama value in the central-thickness cross section (*i.e.*, typical X-ray plane) was equal to 0.1 K$^{1/2}$ s$^{1/2}$ mm^{-1}. An example illustrating this is provided in Figure 14. If the plate shown in this figure was made any longer, the minimum Niyama value would drop below 0.1, and radiographic soundness would no longer be expected. The plate length for which $Ny_{min} = 0.1$ was used to determine the FD, as well as the RZL, and EZL, are shown in Figure 14. The FD rule resulting from this C&LA work is shown in Figure 15, which gives the FD as a function of *W/T*. By dividing FD by the thickness *T* (the dimension into the page for the casting sketch shown in Figure 15), it was possible to represent the FD with a single curve for all section thicknesses in the range being considered. The curve in Figure 15 can be represented by the following polynomial expression:

$$\left(\frac{FD}{T}\right) = -4.29 \times 10^{-4}\left(\frac{W}{T}\right)^4 + 0.0174\left(\frac{W}{T}\right)^3$$
$$-0.266\left(\frac{W}{T}\right)^2 + 1.99\left(\frac{W}{T}\right) + 1.97 \qquad [1]$$
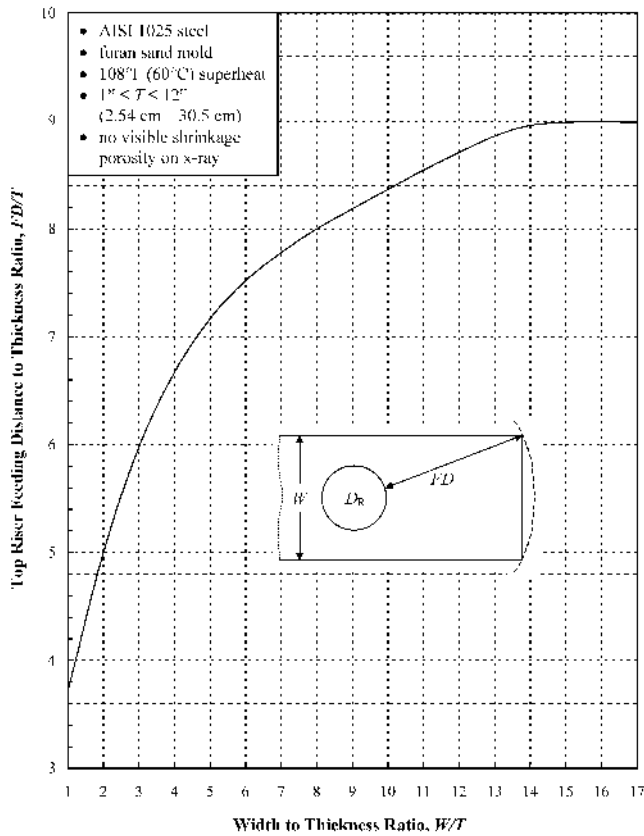
Fig. 15—FD as a function of width and thickness for top-risered sections cast with plain carbon steel.

Table II. Multipliers Used to Apply Base Case Feeding Rules to Other Conditions*

Casting Parameter		Condition Description	Multiplication Factor, C
Sand		furan	1
Mold		green sand	1.09
Material		zircon	0.96
($C_{sand\ mold}$)		chromite	0.88
Cooling		end chill	1.19
Conditions		end effect	1
($C_{cooling\ conditions}$)		drag chill	0.95
Steel Alloy	Carbon	AISI 1025	1
Composition	and Low	AISI 4125	0.98
($C_{cast\ alloy}$)	Alloy	AISI 1522	0.97
		AISI 4135	0.97
		AISI 4330	0.97
		AISI 8620	0.96
		AISI 8630	0.95
		AISI 4340	0.86
	High Alloy	CF8M–C 0.08	1.036
		HH30	0.985
		CF8M–C 0.06	0.978
		HK44	0.965
		CA15–C 0.13	0.943
		HP37	0.904
		CF8M–C 0.03	0.900
Superheat		250 °C	1.38
($C_{superheat}$)		150 °C	1.18
		120 °C	1.12
		90 °C	1.06
		60 °C	1
		30 °C	0.94

*Base case conditions are listed with the multiplier $C = 1$.

Equation [1] is accurate up to $W/T = 15$, beyond which FD/T has a constant value of 9.0.

Figure 15 and Eq. [1] represent the C&LA FD rule for the base case casting conditions, which are

(1) AISI 1025 steel,
(2) PUNB (furan) sand mold, and
(3) 60 °C pouring superheat.

In addition to these base case casting conditions, rules were also developed for different sand mold materials, C&LA steel compositions, pouring superheats, and cooling conditions (end chill, drag chill). It was determined that variations from the base case could all be accounted for with simple multipliers. Then, the FD for casting conditions other than the base case conditions could be computed with the equation

$$\left(\frac{FD}{T}\right)_{different\ conditions} = \left(\frac{FD}{T}\right)_{base\ case} \times C_{superheat} \qquad [2]$$
$$\times C_{cast\ alloy} \times C_{sand\ mold} \times C_{cooling\ conditions}$$

where (FD/T)$_{base\ case}$ represents the FD determined from Figure 15 or Eq. [1], and the multipliers in Eq. [2] are provided in Table II. It should be noted that Eq. [1] was developed for riser-feed casting sections that end in the mold, such as the situation shown in Figure 14 (and the top-view schematic shown in Figure 15). This is termed end-effect feeding. On the other hand, for casting sections that lie between two risers

(termed lateral feeding), a formula analogous to Eq. [1] was developed to determine the lateral FD (LFD). This formula is available in the literature.[10,28] Except for the cooling condition multipliers, all the other multipliers given in Table II can be applied to determine LFDs, if the LFD equation is used for the (FD/T)$_{base\ case}$ in Eq. [2].

For the high-alloy steel rule development, just as in C&LA steels, once the critical minimum Niyama value of 0.1 was determined, a large number of casting simulations were performed for each alloy under consideration (CF-8M, CA-15, HH, HK, and HP). Plate thickness T was again varied from 2.54 to 30.5 cm (1 to 12 in.), and for each thickness, plates were simulated with widths corresponding to $W/T = 1, 2, 4, 6, 8,$ and 12. As in the previous work, the plate length L was varied for each plate until the FD, RZL, and EZL were determined (Figure 14). An example of the results of this effort is shown in Figure 16. This figure contains curves representing FD, RZL, and EZL for CF-8M (0.06 pct carbon). All simulations represented in this figure were performed using furan sand, and a superheat of 100 °C. Again, FD, EZL, RZL, and W are all normalized by the thickness T, so that the FD, RZL, and EZL can each be represented by a single curve for all section thicknesses in the range being considered. By comparing the CF-8M curves in Figure 16 to the CF-8M simulation results for the different thicknesses, one can see that the curves were generated using the average values at each W/T ratio for casting sections with thicknesses ranging from 2.54 to 30.5 cm (1 to 12 in.). Note
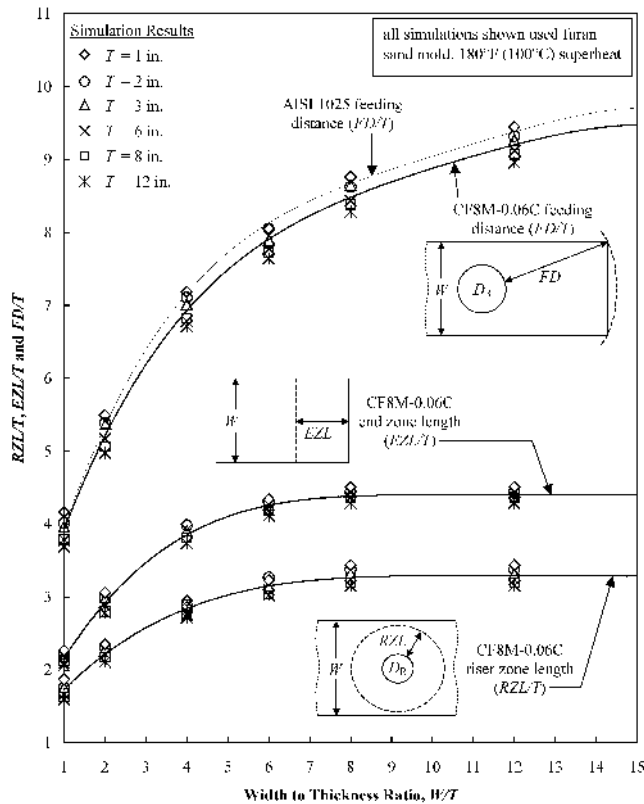
Fig. 16—RZL, EZL, and FD curves for CF-8M (0.06 pct carbon), all normalized by the thickness T, shown with simulation results for various thicknesses.

Fig. 17—FD results for CA-15 (open circles), compared with AISI 1025 feeding distance curve, scaled by 0.943.

that as thickness decreases, FD/T increases slightly. However, it is a relatively small change, and as such, it is neglected for the sake of producing a single FD curve for all values of thickness.

Also shown in Figure 16 is the FD rule for 1025 steel under these casting conditions. Except for the superheat, the conditions for this curve are all the base case conditions (Table II). Therefore, this curve can be determined by multiplying the FD given in Figure 15 or Eq. [1] by the superheat multiplier for 100 °C, which is $C_{superheat} = 1.08$. Notice that this curve and the FD rule for 0.06 pct carbon CF-8M are very similar. In fact, these rules differ by a scale factor; *i.e.*, if the 1025 steel curve is scaled by the factor 0.978 (determined through regression analysis), the result is essentially coincident with the CF-8M curve in this figure. The correlation between these FD curves is possible because the high-alloy rules were developed in a manner completely consistent with the methodology used to develop the C&LA rules. Besides consistent methodology, two other important areas of consistency are worth noting: first, the definitions of FD, RZL, and EZL used for the C&LA and high-alloy rules are identical; and second, the same value of minimum Niyama criterion was chosen as the critical value for both C&LA and high-alloy steels.

Further evidence of the scalability between C&LA and high-alloy FDs is given in Figure 17, which shows the FD results for CA-15, again with furan sand and 100 °C superheat. The open circles represent the average of the simulation results over all thickness values computed at each value of W/T. The upper curve again represents the FD rule for AISI 1025 steel
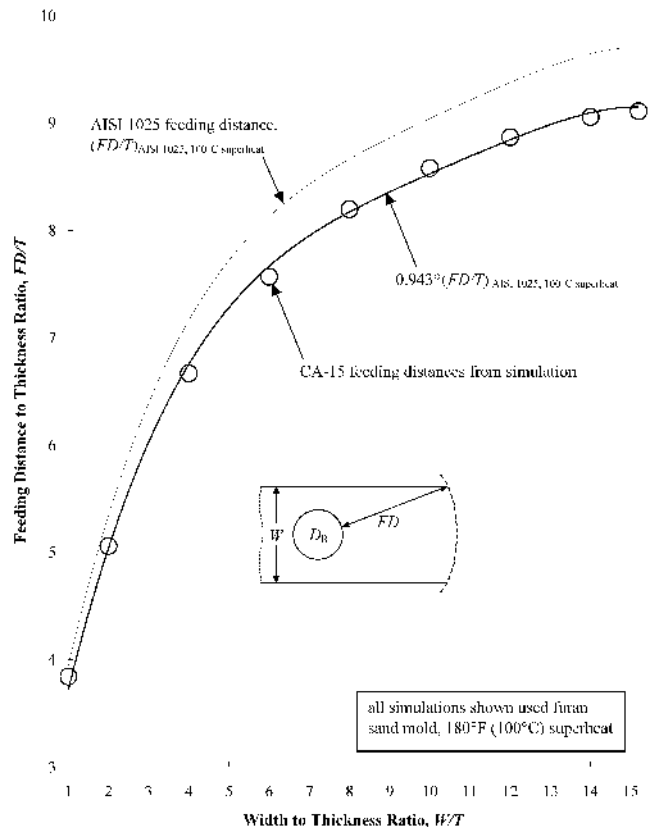
for these casting conditions. The lower curve represents the 1025 curve, scaled by a factor of 0.943 (again determined through regression analysis). Note the good agreement between the scaled 1025 rule and the CA-15 results. This process was repeated for each of the high-alloy grades studied, and the scale factors were collected and tabulated along with the C&LA cast alloy multipliers in Table II. Note that all the high-alloy multipliers are relatively close to unity. The largest deviations from unity, for HP and low-carbon CF-8M, are only 10 pct. This indicates that the FDs of the high-alloy grades considered are all very similar to those of C&LA steels, if all other casting conditions are the same. With the exception of high-carbon CF-8M, all the alloys studied have slightly shorter feeding distances than AISI 1025 steel. In their study, Varga *et al.*[16] found that most of these alloys had longer FDs than C&LA steel. This is likely due to the larger superheats typically used for high-alloy steels than for C&LA steels; pouring temperatures are often similar, but high-alloy steels have significantly lower liquidus temperatures (due to the additional alloying elements) than do C&LA steels. Evidence of the higher superheat can be seen from the data in Table I; the average superheat from the high-alloy casting trials was 158 °C. Considering the superheat multipliers in Table II, a 158 °C superheat has a multiplier of almost 1.2, or a nearly 20 pct increase in FD due to the superheat alone.

As with the C&LA rule development, each high-alloy grade studied was also simulated, over the entire range of T and W/T considered, with superheats ranging from 30 °C to 250 °C, with different sand mold materials, and with drag chills and end

chills. Simulation results were compared with values generated using the end-effect FD rule (Figure 15 or Eq. [1]) with the appropriate multipliers (Eq. [2] and Table II), to ensure that the superheat, mold material, and chill multipliers from the C&LA rule development were also valid for high-alloy steels. An example of this is provided in Figure 18. The middle curve in this figure is the end-effect FD rule for the base casting conditions (Figure 15 or Eq. [1]). The lower curve is the same FD rule scaled by the CF-8M (0.06 pct carbon) multiplier, and the upper curve accounts for both CF-8M and a superheat of 100 °C (180 °F). The open symbols in this plot are simulation results for 5.08-cm (2-in.) thick CF-8M plates cast in furan sand molds; the diamonds represent a superheat of 60 °C, and the circles represent a superheat of 100 °C. Note the good agreement between the simulation results and the corresponding FD rule values. Good agreement was also found for the cooling condition and sand mold material multipliers in Table II.

A comparison between the new high-alloy FD rule and current SFSA rules[26] is provided in Figure 19. The uppermost curve in this figure represents the new FD rule over a range of W/T for CF-8M (0.06 pct carbon) cast in a furan sand mold, with a superheat of 160 °C. As mentioned earlier, this value represents the average superheat from the high-alloy casting trials (Table I); although Varga et al.[16] neither considered nor reported the superheats used in their casting trials, it can be expected that they were of the same order. Again, the new rule was developed using the average FD values for thicknesses ranging from $T = 2.54$ to 30.5 cm (1 to 12 in.), and is valid over this thickness range. The three
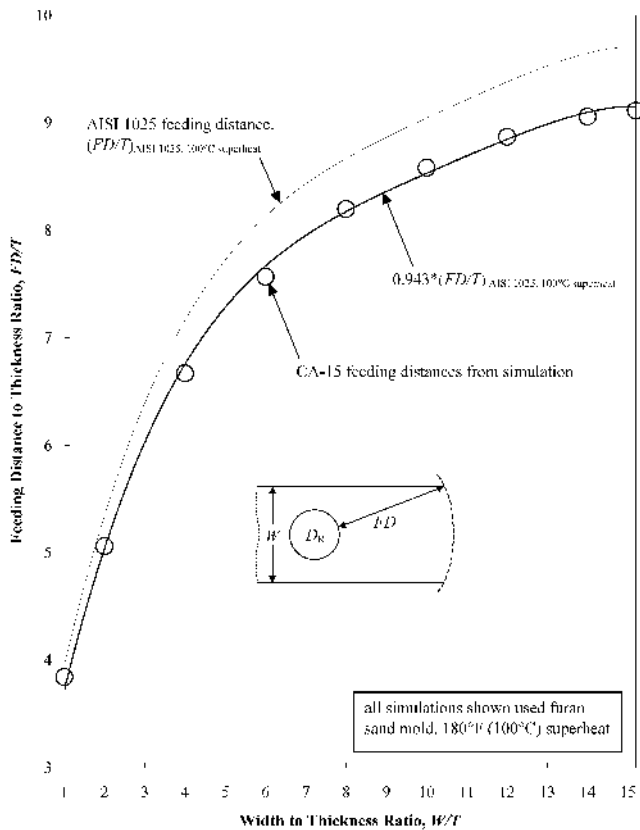
lower curves, which are taken from the high-alloy risering rules in *Risering Steel Castings*,[26] are only applicable to 2.54-cm (1-in.) thick sections. It should be noted that, in *Risering Steel Castings*, there is only one FD rule provided for 2.54-cm (1-in.) thick sections for all the high-alloy grades listed in this figure. However, this handbook measures FD from the center of the riser to the edge of the casting (Figure 1). In order to convert the FD from the SFSA high-alloy definition to the present definition (shown in Figure 19), it is necessary to calculate the appropriate riser size for each casting geometry. *Risering Steel Castings* provides different riser sizing rules for three categories of high-alloy steels; these different rules lead to the three lower curves seen in Figure 19. In this example, the new rule FD is seen to be significantly longer over the entire range of W/T than FDs determined with the existing rules. There are two reasons for this. First, Varga et al.[15–18] developed their rules based solely on empirical analysis; they determined FDs primarily by sectioning castings with centerline shrinkage, and measuring the riser zone (distance from the riser to the beginning of the shrinkage) and end zone (distance from the end of shrinkage to the end of the casting). They added these two values (plus the riser radius) to determine the FD. However, the FD (FD$_{HA}$ in Figure 1) can only be computed as the sum of the riser radius, RZL, and EZL for the longest sound casting before shrinkage forms (e.g., Figure 14). As noted by Pellini and co-workers,[3,6] if the casting length exceeds the maximum length of a sound casting and shrinkage forms (e.g., Figure 10), the shrinkage region

Fig. 18—Comparison between CF-8M (0.06 pct carbon) simulation results and values calculated using FD rule. (FD/T)AISI 1025 is calculated using Eq. [1]; multipliers $C_{CF8M-0.06C}$ and $C_{100\ °C\ superheat}$ are from Table I.
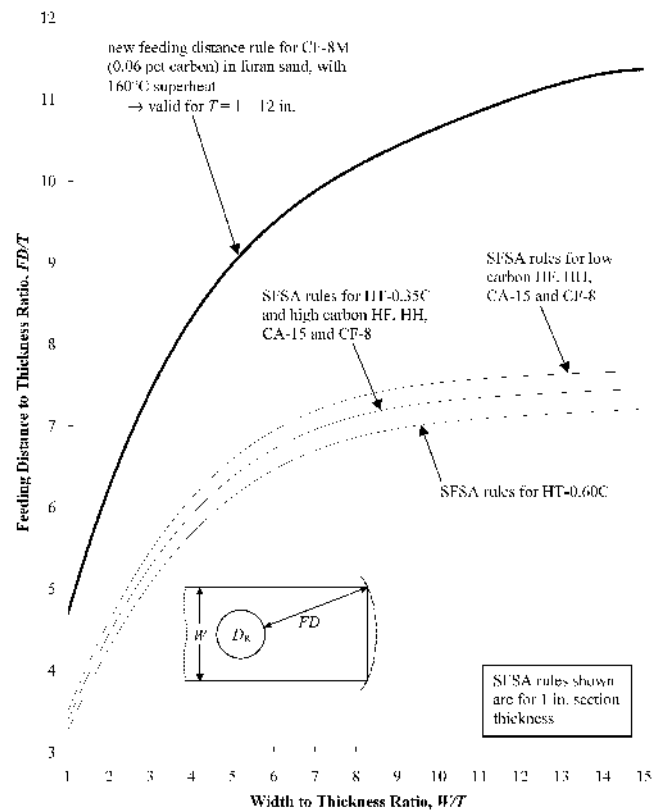
Fig. 19—Comparison between existing rules[26] and the new FD rule for CF-8M (0.06 pct carbon) in furan sand with a 160 °C superheat.

encroaches on the riser zone, which reduces the RZL from its maximum value. This yields a conservative estimate of the FD. Also, *Risering Steel Castings* only provides a single FD chart for all high-alloy grades. Varga *et al.*[16,17] developed such charts for several grades; when this work was condensed into *Risering Steel Castings*, only the most conservative FD chart was provided, so that it would be valid for all alloys.

In summary, through high-alloy casting trials and extensive use of casting simulation, it was determined that the low-alloy FD rules developed in the authors' previous work[9,10,28] are also applicable to the high-alloy grades considered in this work, provided that the appropriate high-alloy grade multiplier (given in Table II) is used. The present work only discussed the end-effect FD rule, applicable to single top risers. However, the previous work also presented rules for lateral feeding and side risers.[10,28] In order to use these lateral feeding or side riser rules for high-alloy steels, one simply needs to replace (FD/T)$_{base\ case}$ in Eq. [2] with the corresponding FD rule, and apply the appropriate multipliers. One clarification is in order, however: if distances are being computed for lateral feeding between two risers, and a drag chill is being used, one should use the end-effect FD rule in Eq. [1] and the drag chill multiplier from Table II to determine this distance. The reason for this is that a drag chill essentially creates an artificial end zone, which approximates an end effect (which is why the drag chill multiplier is close to unity). The end chill and drag chill dimensions recommended for application of these FD rules are given in the previous work.[10,28]

VI. CALCULATION OF RISER SIZE

As stated in Section I, the only known extensive effort to develop riser sizing rules for high-alloy steels was performed by Varga *et al.*;[15–18] this work was later incorporated into the SFSA handbook *Risering Steel Castings*,[26] along with the C&LA riser sizing rules developed by Bishop *et al.*[25] A direct comparison of the C&LA riser sizing rule of Bishop *et al.* and the high-alloy rules of Varga *et al.* is shown in Figure 20. This figure gives the riser-volume-to-casting-volume ratio as a function of the SF of the casting section the riser is intended to feed. From this figure, it is evident that the high-alloy riser sizing rules call for significantly larger riser sizes for a given SF. To understand why this is the case, it is necessary to review how these rules were developed.

Bishop *et al.*[25] developed their C&LA riser sizing rules based on a set of plate casting trials. These trials used open top risers, with a wide range of plate sizes and riser height-to-diameter ratios. Using radiographs of the riser pipe, they defined the minimum riser size as one where the tip of the riser pipe just meets the riser-casting contact surface. Defining the safety margin (SM) to be the distance from the riser-casting contact surface to the tip of the riser pipe (Figure 21), the minimum riser requirement of Bishop *et al.* can also be described as a riser having a SM of zero (SM = 0). Through experimentation, they found that the minimum riser height could be determined from any casting by determining its SM, provided that the SM did not exceed 1 or 2 in. The minimum riser height was found by simply subtracting the SM from
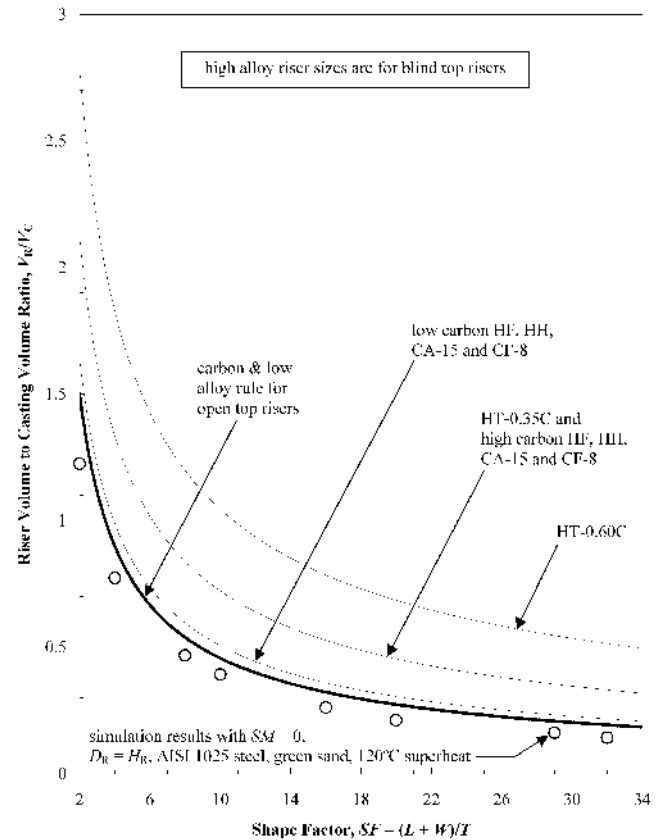

Fig. 20—Direct comparison between the C&LA riser sizing rules of Bishop *et al.*[25] and the high-alloy riser sizing rules of Varga *et al.*[16]
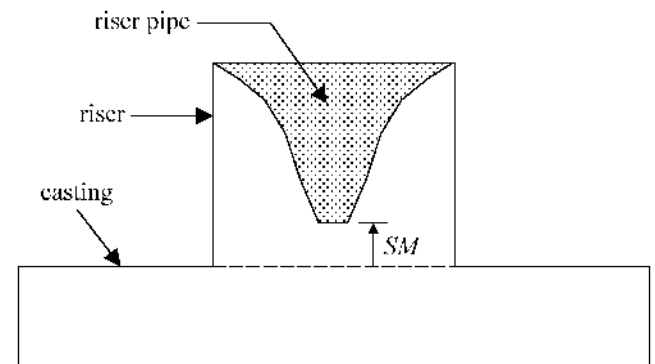

Fig. 21—Sketch illustrating the definition of SM.

the original riser height (*i.e.*, $H_{R,min} = H_R − SM$). Note that if the riser pipe extended into the casting, the SM was negative, so the minimum riser height was larger than the original height. Bishop *et al.* used this new minimum riser height ($H_{R,min}$) with the original riser diameter (D_R) to determine the minimum riser volume, and in this manner developed a plot of riser-volume-to-casting-volume ratio *vs* SF. The experimental data in this plot fall in a band of riser volumes for each SF; Bishop *et al.* included an upper-bound curve (above which the riser is too large) and a lower-bound curve (below which the riser is too small) for the experimental data. The C&LA riser size curve shown in Figure 20, developed by Spiegelberg,[12] represents the upper-bound curve of this band.

The nomograph given to size C&LA in *Risering Steel Castings*[26] was developed from this upper-bound curve. Note that by choosing the upper-bound curve of this band, a slight factor of safety is included in this riser-sizing curve.

Varga *et al.*[15,16] developed their high-alloy riser sizing rules using methodology similar to that of Bishop *et al.*, but with several important differences. They also performed casting trials, for the high-alloy steels they were investigating, and used riser pipe radiographs to determine the SM. For their study, however, all of their risers were blind top risers (both with and without cracker cores) that had height-to-diameter ratios of unity (*i.e.*, $D_R = H_R$). When they measured the SM, then, they modified both the riser height and diameter to determine the minimum riser size (*i.e.*, $H_{R,\min} = H_R - SM$ and $D_{R,\min} = D_R - SM$). An important note regarding this procedure, however, is that most of their original risers were too small. As a result, most of their riser pipes extended into the castings (up to about 1.27 cm (0.5 in.)), producing negative safety margins, as illustrated in Figure 22. Thus, when they calculated minimum riser size, they typically increased
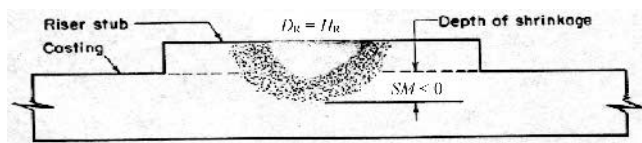
both the riser height *and* diameter, when it was really only necessary to increase the height (according to the methodology experimentally established by Bishop *et al.*[25]). This produced larger than necessary riser volumes.

Also analogous to Bishop *et al.*, Varga *et al.* then plotted the experimental minimum riser volumes as a function of SF. The results for each alloy grade were plotted separately, and if the alloy was cast both with and without cracker cores, two plots were made for that alloy grade to separate this effect as well. Varga *et al.* then represented the band of experimental data in each of these plots by using the upper-bound curve, analogous to the C&LA curve shown in Figure 20. When an alloy grade had results both with and without cracker corse, they condensed this information by using the more conservative of the two to represent that alloy grade. The results for blind risers with cracker cores were selected, as they tend to produce deeper riser pipes. This is illustrated through MAGMASOFT casting simulation results in Figure 23. This figure shows riser pipes for a 2.54 by 38.1 by 35.6 cm (1 by 15 by 14 in.) CA-15 plate casting with a riser having both diameter and height equal to 7.64 cm (2.9375 in.). Note that the open riser has a larger SM than either blind riser case. The blind riser with the cracker core has a slightly deeper riser pipe than the vented blind riser without a cracker core; this trend is seen in industry as well. However, the difference between the riser pipes in Figures 23(b) and (c) is small enough that it could be considered a grid effect; a finer grid would be required to verify this difference. Figure 23(c) corresponds to one of the plates cast in the trials of Varga *et al.*; they
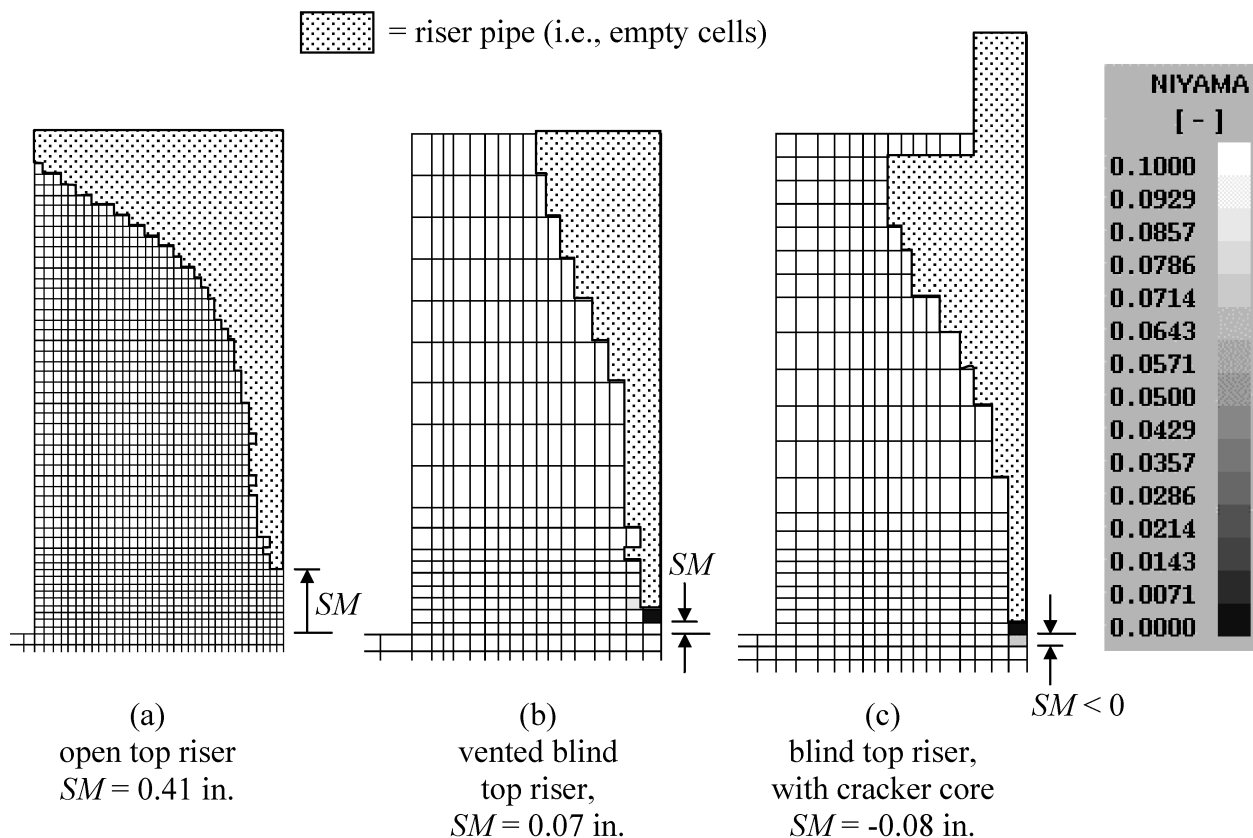

Fig. 22—Illustration of negative SM due to insufficient riser size. Reproduced from Varga *et al.*[16]

(a)
open top riser
SM = 0.41 in.

(b)
vented blind
top riser,
SM = 0.07 in.

(c)
blind top riser,
with cracker core
SM = -0.08 in.

Fig. 23—Comparison of SMs for a CA-15 plate casting with different types of risers.

measured a SM of −0.76 cm (−0.3 in.). The discrepancy between the measured value and the simulated value of −0.20 cm (−0.08 in.) is likely due to the fact that Varga *et al.* did not report the superheat used to produce these plates; a superheat of 150 °C was used in the simulations shown in Figure 23; however, if a superheat of 200 °C is used in the case shown in Figure 23(c), the simulated SM is −0.69 cm (−0.27 in.). It should be noted that the riser pipes simulated by MAGMASOFT[32] have been verified to be accurate. MAGMASOFT predicts the riser pipe by computing the shrinkage during solidification, and then lowering the liquid metal surface in the riser accordingly to conserve mass. A comparison between simulations and the casting trial results of Bishop *et al.*[25] (who did report superheats) for 1025 steel castings is shown in Figure 24. The good agreement between simulated and measured SMs seen in this figure is typical of the many comparisons of this type that were performed in the course of this high-alloy work, as well as in similar comparisons made for other projects. Finally, two other factors of safety were built into the riser sizing rules of Varga *et al.* First, they combined the alloys they considered into three groups (the three high-alloy groups shown in Figure 20), taking the most conservative curve from each group to represent the entire group. Finally, when they had reduced their data down to riser sizing curves for three groups, they increased the riser sizes further by adding a safety margin of 0.64 cm (0.25 in.) to define their minimum riser size.

Also shown in Figure 20 (as open circles) are simulation values of the minimum riser size for several SFs. These simulations were performed with AISI 1025 steel in a green sand mold, with a 120 °C superheat. All risers in the simulations were open top risers with height-to-diameter ratios of unity, and the minimum riser size was defined as a riser with SM = 0. This was determined by iteratively changing the riser size until the simulation resulted in a zero safety margin. Note that the simulation data agree very well with the C&LA riser sizing curve of Bishop *et al.*, and that the simulation data are slightly less conservative. This is not surprising, considering that the C&LA curve shown was taken as the upper-bound curve from the SM = 0 data in the work of Bishop *et al.*

As stated earlier, the C&LA riser sizing rule developed by Spiegelberg,[12] based on the work of Bishop *et al.*,[25] is considered adequate for C&LA steels. The changes made by Varga *et al.*[15,16] in the methodology of Bishop *et al.* result in riser sizing rules that are too conservative. In an effort to demonstrate this, the minimum riser sizes for the casting trial data of Varga *et al.* were recalculated, using the same riser sizing methodology that was used by Bishop *et al.* (*i.e.*, determining the minimum riser dimensions by changing the riser height based on the safety margin, but continuing to use the original riser diameter, and also, by designing the minimum riser size for SM = 0 rather than 0.64 cm (0.25 in.)). The results for each alloy were combined into the same groups used by Varga *et al.*, taking the most conservative results from each group. This information is plotted in Figure 25. Comparing Figure 25 to Figure 20, note that the recalculated high-alloy blind riser sizes are considerably less conservative than those of Varga *et al.* The results for low-carbon HF, HH, CA-15, and CF-8 are, in fact, nearly coincident with the C&LA curve for open top risers. The curves for the other high-alloy
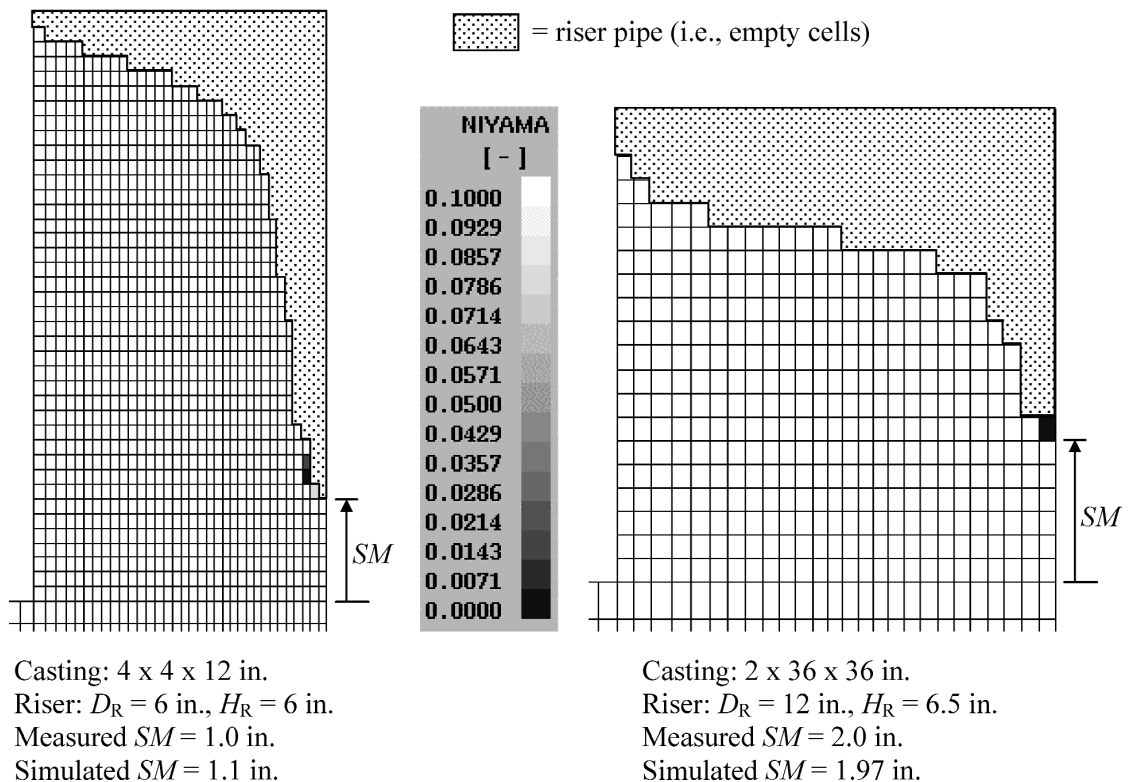

= riser pipe (i.e., empty cells)

NIYAMA [-]

0.1000
0.0929
0.0857
0.0786
0.0714
0.0643
0.0571
0.0500
0.0429
0.0357
0.0286
0.0214
0.0143
0.0071
0.0000

Casting: 4 x 4 x 12 in.
Riser: D_R = 6 in., H_R = 6 in.
Measured SM = 1.0 in.
Simulated SM = 1.1 in.

Casting: 2 x 36 x 36 in.
Riser: D_R = 12 in., H_R = 6.5 in.
Measured SM = 2.0 in.
Simulated SM = 1.97 in.

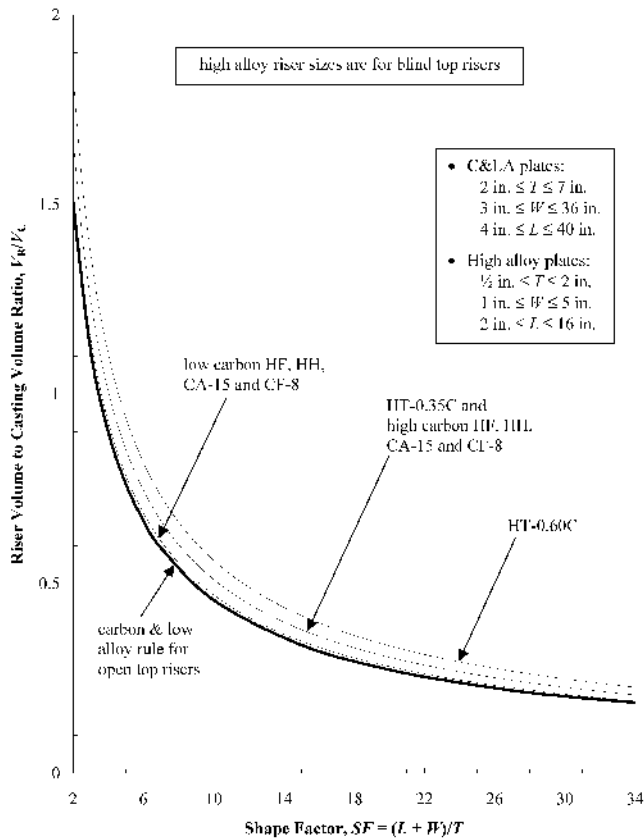Fig. 24—Comparison between simulated SMs and measured values from Bishop *et al.*[25] for 1025 steel.

Fig. 25—Comparison between the C&LA riser sizing rules of Bishop *et al.*[25] and the high-alloy riser sizing rules of Varga *et al.*,[16] if the high-alloy rules are sized according to the methodology of Bishop *et al.*

Fig. 26—Minimum riser sizes (based on a safety margin of zero) for various alloys.

grades are not very far above the C&LA curve for open top risers.

The issue of whether different riser sizing curves are truly required for different high-alloy grades was investigated further. As mentioned in the discussion of Figure 9(b), due to the differences in density curves among the alloy grades, the differences in their solidification shrinkage can be significant. This could indicate that riser pipe depths may be different for different alloys, and that different riser sizes for the same casting section may be required. However, as illustrated in Figure 26, simulation results indicate that this is not the case. This figure shows minimum riser sizes for simulations of plate castings of various sizes and alloys. All other casting conditions were held constant for these simulations. As with the simulation results shown in Figure 20, the minimum riser sizes were calculated using open top risers with $H_R/D_R = 1$, and iterating on the riser size until a SM of zero was achieved. Here, the alloys CF-3 and CF-20 are included (although they were not used in the plate casting trials) because they represent extremes in solidification shrinkage, and AISI 1025 is included along with the high-alloy grades for comparison. Notice that the minimum riser sizes for a given plate size are essentially constant, regardless of the alloy. This indicates that, for open top risers, as long as the casting conditions other than alloy grade are held constant, the same size riser can be used, regardless of the alloy. Therefore, the C&LA curve shown in Figure 25 can be used to size high-alloy open top risers as well as C&LA open top risers.
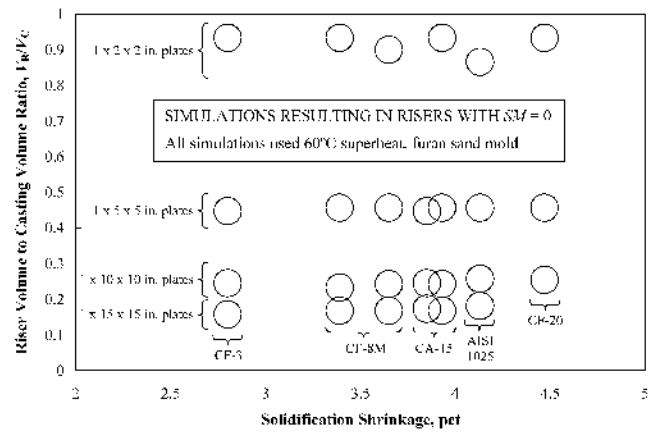
Figure 27 explains why the same riser size can be used for different alloys, even though their solidification shrinkage varies from 2.8 to 4.5 pct (Figure 26). This figure shows the predicted riser pipes for six different alloys cast under the same conditions. All of the simulations are for a 2.54 by 12.7 by 35.6 cm (1 by 5 by 14 in.) plate, with a vented blind top riser [$D_R = 6.70$ cm (2.6375 in.) and $H_R = 7.46$ cm (2.9375 in.)], cast in a green sand mold, with a 100 °C superheat. It can be seen that the SM for all these risers is essentially the same. However, the riser pipes have different shapes: some are wider and some are narrower. To understand why the riser pipes have different shapes but about the same depth, consider how a riser pipe forms. As the casting solidifies, feed metal is drawn from the riser into the casting, and the riser free surface lowers accordingly. The riser will also begin to solidify, beginning with the outside (cylindrical) surface of the riser and moving inward toward the cylindrical center of the riser. As solidification proceeds, the liquid free surface of the riser shrinks in concentric circles, while simultaneously lowering as more feed metal is drawn from the riser to the casting. In alloys with larger solidification shrinkage percentages (*e.g.*, CF-20), the riser surface drops more rapidly, particularly early in solidification when shrinkage occurs more rapidly (Figure 9). This results in a wider riser pipe, because the surface drops while the liquid free surface of the riser is still large. The wider liquid channel feeds a larger volume of metal into the casting than do the narrower channels of alloys with smaller solidification shrinkage percentages (*e.g.*, CF-8M 0.06C). Later in solidification, the narrow liquid channels of smaller solidification shrinkage alloys must drop faster to accommodate the shrinkage volume (due to their small surface area) than the wider channels of larger solidification shrinkage alloys, which are still able to provide more feed metal due simply to their larger liquid surface area. These phenomena, coupled with the very similar thermal conditions for all of these castings (similar freezing ranges, as shown in Figure 9(a), and the same superheat), combine to produce riser pipes that have the same depth, but with different volumes to accommodate different amounts of shrinkage. This indicates that the size of risers can generally be chosen independently of alloy grade for the C&LA steels and the high-alloy grades considered.
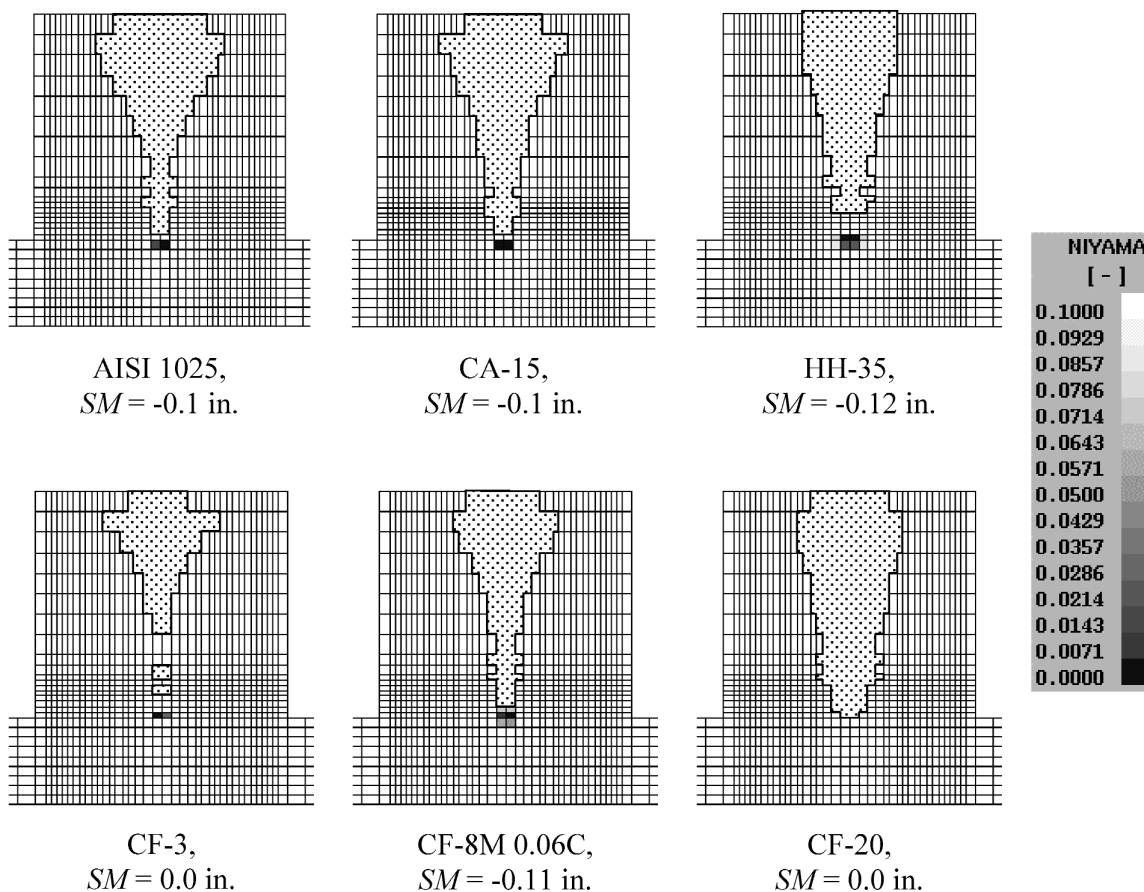
Fig. 27—Comparison between riser pipes of different steel alloys. All risers shown are vented top blind risers.

In summary, based on this work, the following riser sizing recommendations are made for the high-alloy steel grades considered:

(1) For open top risers: size the riser using the C&LA riser sizing rule given in Figure 25.
(2) For blind top risers: although the casting trials performed in this work did not use blind risers, simulation with vented blind top risers indicates that the size of blind risers is also independent of the alloy grade, for the high-alloy grades considered. Although no blind riser rule was developed, the same practice used in C&LA foundries can be employed: size the riser based on the C&LA rule for open top risers, and then make the riser somewhat taller to account for the deeper pipe that results from a blind riser.

VII. CONCLUSIONS

A new set of FD and riser sizing rules has been developed for high-alloy steel grades CF-8M, CA-15, HH, HK, and HP. By comparing casting trial results with corresponding casting simulation results, a correlation was developed between the Niyama criterion (a local thermal parameter) and casting soundness. Using this information, extensive casting simulation was used to develop FD rules for a wide range of casting condi-

tions. It was found that the FD rules developed in an earlier analogous study for carbon and low-alloy steels could also be used for the high-alloy steels considered, provided that the FD was modified by the appropriate high-alloy steel grade multiplier. Other multipliers for these FD rules account for superheat, sand mold material, and the use of chills. The new high-alloy FD rules, which are valid for section thicknesses ranging from 2.54 to 30.5 cm (1 to 12 in.), are shown to be less conservative than existing FD rules, and are more tailored to the actual casting conditions. In another part of this study, high-alloy riser sizing rules were investigated. It was determined that if open top risers are used, the C&LA riser sizing rule (which is less conservative than previously published high-alloy riser sizing rules) is applicable for high-alloy steels as well. This study also determined that riser size is independent of alloy grade for blind top risers.

their work in helping organize the trials and recruiting members to participate. Most importantly, we thank the participants in the plate casting trials for their substantial investments of both time and resources. This work could not have been accomplished without their shared efforts.

REFERENCES

1. Steel Founders' Society of America Special Report No. 30, SFSA, Crystal Lake, IL, 1998.
2. C. Beckermann, X. Shen, J. Gu, and R.A. Hardin: *1997 SFSA Technical and Operating Conf.*, SFSA, Crystal Lake, IL, 1997.
3. H.F. Bishop and W.S. Pellini: *Am. Foundrymen's Soc. Trans.*, 1950, vol. 58, pp. 185-97.
4. H.F. Bishop, E.T. Myskowski, and W.S. Pellini: *Am. Foundrymen's Soc. Trans.*, 1951, vol. 59, pp. 171-80.
5. E.T. Myskowski, H.F. Bishop, and W.S. Pellini: *Am. Foundrymen's Soc. Trans.*, 1952, vol. 60, pp. 389-400.
6. W.S. Pellini: *Am. Foundrymen's Soc. Trans.*, 1953, vol. 61, pp. 61-80.
7. E.T. Myskowski, H.F. Bishop, and W.S. Pellini: *Am. Foundrymen's Soc. Trans.*, 1953, vol. 61, pp. 302-08.
8. C.W. Briggs: Steel Founders' Society of America Research Report No. 30, Technical Research Committee Report, SFSA, Crystal Lake, IL,1953.
9. K.D. Carlson, S. Ou, R.A. Hardin, and C. Beckermann: *Metall. Mater. Trans. B*, 2002, vol. 33B, pp. 731-40.
10. S. Ou, K.D. Carlson, R.A. Hardin, and C. Beckermann: *Metall. Mater. Trans. B*, 2002, vol. 33B, pp. 741-55.
11. W.D. Spiegelberg: Master's Thesis, Case Western Reserve University, Cleveland, OH, 1968.
12. W.D. Spiegelberg: Ph.D. Thesis, Case Western Reserve University, Cleveland, OH, 1970.
13. R. Maier: Master's Thesis, Case Western Reserve University, Cleveland, OH, 1972.
14. W.P. Ghun: Master's Thesis, Case Western Reserve University, Cleveland, OH, 1974.
15. J. Varga, Jr. and H.W. Lownie, Jr.: "Summary Report on Solidification and Feeding of High-Alloy Castings," Alloy Casting Institute, Apr. 1955.
16. J. Varga, Jr., A.J. Stone, and H.W. Lownie, Jr.: "Summary Report on Solidification and Feeding of High-Alloy Castings," Alloy Casting Institute, Sept. 1956.
17. J. Varga, Jr., A.J. Stone, and H.W. Lownie, Jr.: "Summary Report on Solidification and Feeding of High-Alloy Castings," Alloy Casting Institute, Sept. 1957.
18. J. Varga, Jr., A.J. Stone, and H.W. Lownie, Jr.: "Summary Report on Solidification and Feeding of High-Alloy Castings," Alloy Casting Institute, June 1958.
19. N. Chvorinov: *Giesserei*, 1940, vol. 27, pp. 177-225.
20. N. Janco: *Am. Foundrymen's Soc. Trans.*, 1947, vol. 55, pp. 296-300.
21. N. Chvorinov: *Foundry Trade J.*, 1939, pp. 95-98.
22. Wlodawer: *Directional Solidification of Steel Castings*, 1st English ed., Pergamon Press Inc., Long Island, NY, 1966, pp. 1-15.
23. R.W. Ruddle: *Am. Foundrymen's Soc. Trans.*, 1971, vol. 79, pp. 269-80
24. J.B. Caine: *Am. Foundrymen's Soc. Trans.*, 1949, vol. 57, pp. 492-501.
25. H.F. Bishop, E.T. Myskowski, and W.S. Pellini: *Am. Foundrymen's Soc. Trans.*, 1955, vol. 63, pp. 271-81.
26. *Risering Steel Castings*, Steel Founders' Society of America, Crystal Lake, IL, 1973.
27. E. Niyama, T. Uchida, M. Morikawa, and S. Saito: *Am. Foundrymen's Soc. Int. Cast Met. J.*, 1982, vol. 7(3), pp. 52-63.
28. *Feeding & Risering Guidelines for Steel Castings*, Steel Founders' Society of America, Crystal Lake, IL, 2001.
29. ASTM E94-00, *Annual Book of ASTM Standards*, vol. 03.03, *Nondestructive Testing*, ASTM, Philadelphia, PA, 2002.
30. ASTM E446-98, *Annual Book of ASTM Standards*, vol. 03.03, *Nondestructive Testing*, ASTM, Philadelphia, PA, 2002.
31. K. Carlson, S. Ou, R.A. Hardin, and C. Beckermann: *Int. J. Cast Met. Res.*, 2001, vol. 14 (3), pp. 169-83.
32. *MAGMASOFT*, MAGMA GmbH, 52072 Aachen, Germany.
33. *AFSolid*, AFS, Inc., Des Plaines, IL.
34. Steel Founders' Society of America Research Report No. 110, SFSA, Crystal Lake, IL, 2001.
35. J. Miettinen: *Metall. Mater. Trans. B*, 1997, vol. 28B, pp. 281-97.
36. J. Miettinen and S. Louhenkilpi: *Metall. Mater. Trans. B*, 1994, vol. 25B, pp. 909-16.
37. B. Carlsson and B. Callmer: *A Guide to the Solidification of Steels*, Jernkontoret, Stockholm, 1977.